



Neoproterozoic granitoids of northwest Vietnam and their tectonic implications

Ngo Xuan Dac^{a,b}, Asad Khan^c, Zaheen Ullah^d, Trinh Hai Son^a, Li Xiao Chun^e, Khuong The Hung^b, Guanzhong Shi^f, Duan Zhuang^g and Muhammad Farhan^h

^aDepartment of Mineral Resources, Vietnam Institute of Geosciences and Mineral Resources, Hanoi, Vietnam; ^bDepartment of Mineral Resource Prospecting and Exploration, Hanoi University of Mining and Geology, Hanoi, Vietnam; ^cDepartment of Geology, FATA University, FR Koah, Pakistan; ^dCentre for Earth and Space Sciences, University of Swat, Swat, Pakistan; ^eKey Laboratory of Mineral Resources, Institute of Geology and Geophysics, Chinese Academy of Sciences, Beijing, China; ^fKey Laboratory of Tectonics and Petroleum Resources, China University of Geosciences, Wuhan, China; ^gInstitute of Geophysical and Geochemical Exploration, Chinese Academy of Geological Sciences, Langfang, Hebei, China; ^hDepartment of Marine Sciences, Zhejiang University, Zhoushan, China

ABSTRACT

A combined study of whole-rock geochemical and Sr-Nd isotopic data, and zircon U-Pb geochronological and Hf isotopes has been carried out for several Neoproterozoic intrusions, including the Lung Thang, Posen and Sin Quyen in the Phan Si Pan Zone, northwest Vietnam to constrain their age, petrogenesis and tectonic implications. The Lung Thang and Posen intrusions, mainly composed of granodiorite, were formed at 803–777 Ma and are characterized by moderate SiO₂ (64.43–66.65 wt.%), and K₂O (4.05–4.89 wt.%), with A/CNK and A/NK values of (0.94–1.03) and (1.72–2.11), respectively. They have negative whole-rock $\epsilon_{Nd}(t)$ (–6.16 to –3.73) and zircon $\epsilon_{Hf}(t)$ values (–7.9 to –4.1), which suggest that the Lung Thang and Posen intrusions were generated by partial melting of ancient, K-rich crustal rocks. The Sin Quyen intrusion, occurring as dykes, is composed of monzodiorite and was emplaced at 742 ± 3 Ma. The Sin Quyen intrusion has high alkalis (K₂O+Na₂O = 7.42–7.47 wt.%), and low MgO (<1.31 wt.%) and Ni (6.55–6.93 ppm), with A/CNK and A/NK values of (0.67–0.68) and (1.64–1.68), respectively. Their whole-rock $\epsilon_{Nd}(t)$ and zircon $\epsilon_{Hf}(t)$ values are –6.15 to –5.92 and –5.8 to +8, respectively. These geochemical characteristics suggest that the Sin Quyen intrusion was produced by the partial melting of ancient crustal sources mingled with mantle-derived components. Geochemically, the Lung Thang, Posen and Sin Quyen intrusions are medium- to high-K, calc-alkaline in nature and show enrichment in LILE (Th, U, K, Rb) and LREE, and strong negative anomalies of Nb, Ta, and Ti. Such geochemical characteristics suggest that they formed in a subduction-related tectonic environment. The geochronological and geochemical correlation of these intrusions with those along the southwestern margin of the Yangtze Block in South China suggests that the Phan Si Pan zone in northwestern Vietnam is a constituent of the SW Yangtze Block. Additionally, these intrusions show a significant correlation with other contemporaneous magmatic rocks in the northeast Indochina Block, Lhasa Block, the northwestern margin of Greater India as well as those in Seychelles and northern Madagascar. This correlation suggests a similar history and synchronous episode of crustal growth/recycling in an Andean-type arc system along the western and northern margin of the Rodinia supercontinent during the Neoproterozoic.

ARTICLE HISTORY

Received 4 August 2023
Accepted 20 January 2024




KEYWORDS


Geochemistry; Zircon U-Pb-hf isotopes; Neoproterozoic, northwest Vietnam; Rodinia


1. Introduction

Granitoids are the main constituents of the continental crust, and thus offer an important understanding of the crustal evolution and tectonic history (Jahn *et al.* 2000; Ashwal *et al.* 2002, 2013; Zhou *et al.* 2006, 2006; Pham *et al.* 2012; Rehman *et al.* 2021; Zhao *et al.* 2021). Granitoids in continental arcs may characterize the subduction process of oceanic lithosphere beneath continental plate (Qi *et al.* 2014, 2016; Moghadam *et al.* 2015; Pereira *et al.* 2015; Faisal *et al.* 2016; Li *et al.* 2018; Sajid *et al.* 2018), which provide important constraints on the

subduction history and the amalgamation of continents and supercontinents (Ashwal *et al.* 2002, 2013; Zhou *et al.* 2006, 2006; Pham *et al.* 2012; Qi *et al.* 2014, 2016; Li *et al.* 2018; Mastoi *et al.* 2020; Baig *et al.* 2021; Rehman *et al.* 2021). The South China and Indochina blocks are important integral components in the palaeogeographic reconstruction of the Rodinia supercontinent (Metcalf 2002, 2006; Lepvrier *et al.* 2004; Boger 2011; Johnson *et al.* 2011). Previous studies have reported widely distributed Neoproterozoic granitoids in the Panxi-Hannan Belt and Jiangnan Orogen of the South China Block,

CONTACT Asad Khan  asadgeo89@gmail.com  Department of Geology, FATA University, FR Koah, Pakistan; Ngo Xuan Dac  dacbmks@gmail.com

 Vietnam Institute of Geosciences and Mineral Resources, Hanoi, Vietnam

 Supplemental data for this article can be accessed online at <https://doi.org/10.1080/00206814.2024.2309470>

© 2024 Informa UK Limited, trading as Taylor & Francis Group

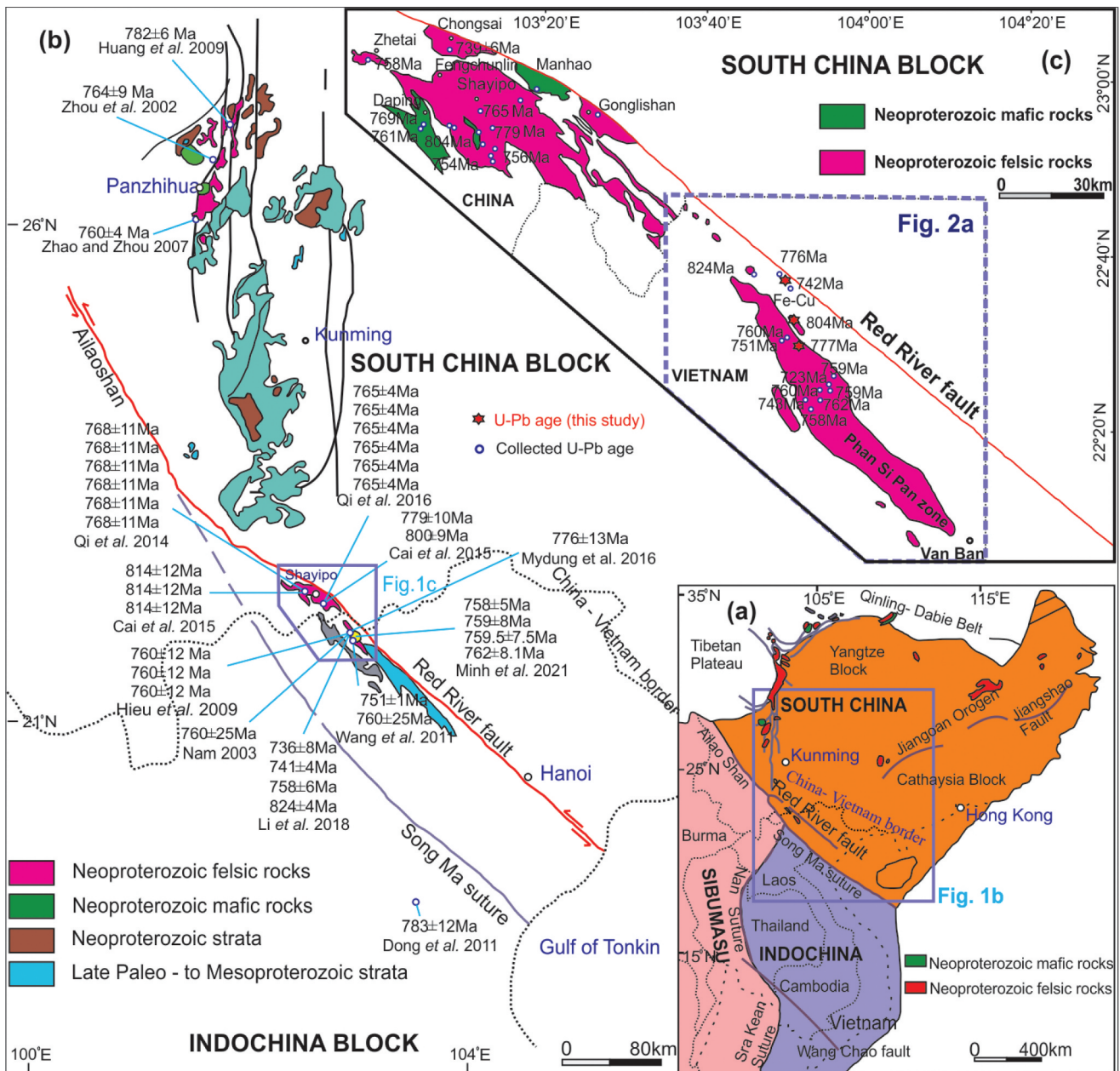


Figure 1. Simplified tectonics map of NW Vietnam and adjoining areas (Pham *et al.* 2009; Wang *et al.* 2016; Qi *et al.* 2016; Minh *et al.* 2021 and references therein).

as well as Phan Si Phan Zone in NW Vietnam (Figure 1a) (Pham *et al.* 2009; Qi *et al.* 2014, 2016; Yang *et al.* 2016; Cawood *et al.* 2018), and various tectonic models have been proposed to interpret the tectonic settings of these granitoids, such as rift setting (Zheng *et al.* 2008), subduction setting (Zhao and Zhou 2007; Pham *et al.* 2009; Huang *et al.* 2009; Zhao *et al.* 2011; Qi *et al.* 2014, 2016), and intracontinental orogeny (Shu *et al.* 2011). Given the uncertain interpretations of the tectonic setting of this magmatism, the positioning of the South China Block within Rodinia is also a subject of significant debate,

including external or internal position models (Cawood *et al.* 2020 and references therein).

Recently, the Neoproterozoic magmatic rocks found in the Phan Si Pan Zone, Northwest Vietnam, have been studied by several researchers (Nam *et al.* 2003; Pham *et al.* 2009; Wang *et al.* 2011; Qi *et al.* 2014, 2016). However, the origin of these Neoproterozoic magmatic rocks in the Phan Si Pan Zone remains a subject of ongoing debate. Lan *et al.* (2000) suggested that these Neoproterozoic rocks originated through partial melting of the ancient crust, accompanied by limited contribution of mantle material, while other geologists suggest

that these rocks exhibit adakitic characteristics, indicative of partial melting of ancient oceanic crust within a subduction zone setting (Li *et al.* 2018; Minh *et al.* 2021 and References therein). While progress has been made in understanding the magmatic evolution of these Neoproterozoic rocks, there remains a need to establish more precise constraints on the evolution of magmatism and the associated Neoproterozoic tectonic evolution within Rodinia. Furthermore, there is still debate regarding the tectonic affinity of Northwest Vietnam. Qi *et al.* (2012, 2014). suggest that Northwest Vietnam is tectonically affiliated with Indochina Block. Alternatively, the Phan Si Pan Zone in northwest Vietnam is considered to be a part of the southwestern Yangtze Block (Li *et al.* 2018; Zhou *et al.* 2020; Minh *et al.* 2021). Thus, some researchers suggest that the Phan Si Pan Zone in northwest Vietnam is an important, albeit poorly studied, segment of the Panxi-Hannan Belt of the west-southwestern Yangtze Block (Li *et al.* 2018; Minh *et al.* 2021). In the Panxi-Hannan Belt, the Neoproterozoic magmatic rocks are distributed in Panzhihua and Shayipo in the Yangtze Block (Zhao and Zhou 2007; Huang *et al.* 2009) (Figure 1b,c). These rocks formed from ca. 900 Ma to ca. 700 Ma and were proposed to have been generated under tectonic settings of subduction or rifting related to the amalgamation and break-up of Rodinia (Ao *et al.* 2019; Zou *et al.* 2021). Thus, the Neoproterozoic tectonic setting of the Phan Si Pan Zone is controversial, which has affected our understanding of NW Vietnam as well as the Panxi-Hannan Belt in SW and west Yangtze Block.

In order to provide a better understanding of the petrogenesis, emplacement and tectonic setting of

Neoproterozoic magmatic rocks as well as the Neoproterozoic crustal evolution in the Phan Si Pan Zone, we have investigated geochemistry, U-Pb zircon geochronology, and Sr-Nd-Hf isotopic compositions of Lung Thang, Posen and Sin Quyen granitoids in the region. By integrating our data with other published regional geological records, we can enhance our understanding of (1) the timing of the emplacement of these granitoids, (2) constrain their petrogenesis and tectonic setting and (3) advance our understanding of the correlation between Neoproterozoic magmatism in northwest Vietnam and their linkage with other major continents within the Rodinia supercontinent.

2. Geological setting

Northwest Vietnam is bounded by the Song Chay fault to the north, and the Song Ma belt to the south (Figure 2a). Three major tectonic units exist in Northwest Vietnam, namely the Phan Si Pan Zone, Song Da rift and Tu Le basin (Figure 2a). The Song Da rift is a northwest-southeast oriented, lozenge-shaped region and mainly consist of Devonian to Middle Triassic sedimentary-volcanic sequences. Well-developed Permo-Triassic alkaline basalts (~260 Ma) are significant in the Song Da rift, mainly along the Da River (Polyakov *et al.* 1998). These alkaline basalts and silicic volcanic rocks overlie early Permian limestone and are overlain unconformably by Triassic limestone and shale-containing coal (Anh *et al.* 2011; Metcalfe 2012). Some researchers consider the Song Da volcanic suite related to the Emeishan

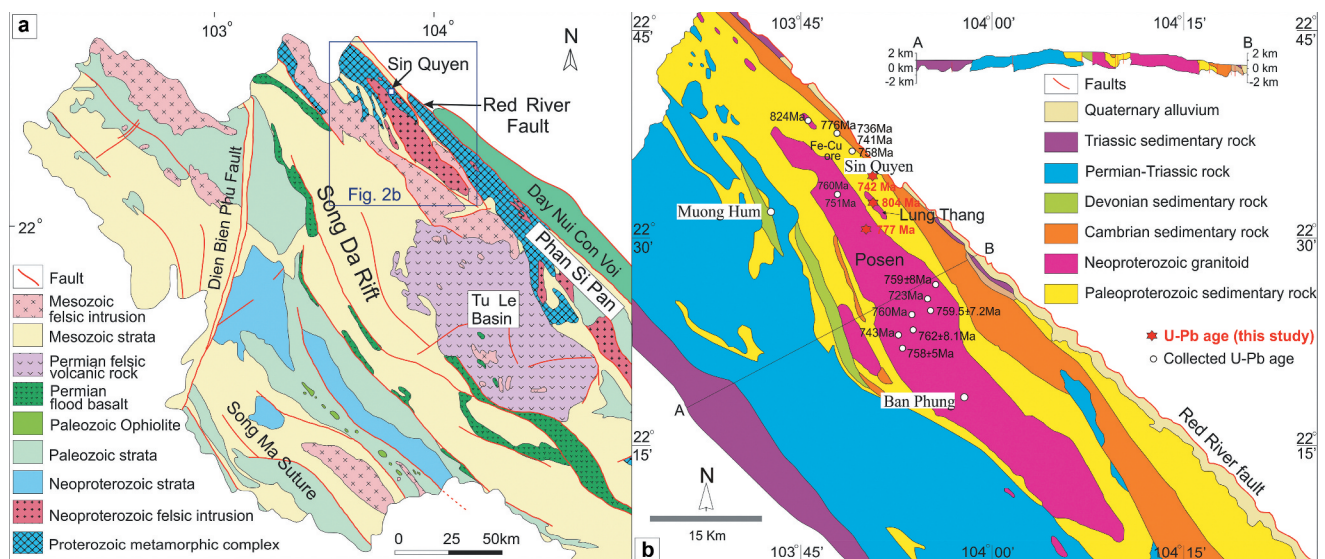


Figure 2. Geological map of (a) northwestern Vietnam and (b) the Phan Si Pan zone (modified after DGMVN 1995). The geochronological data is from Nam *et al.* (2003); Pham *et al.* (2009); Wang *et al.* (2011); Li *et al.* (2018) and this study.

plume (Faure *et al.* 2014, 2016; Minh *et al.* 2018). The Tu Le basin consists dominantly of rhyolite, trachyrhyolite and trachydacite. Zircon U-Pb dating show that rhyolites in the Tu Le basin are Late Permian (262–252 Ma), which is contemporaneous with the mafic rocks of the Song Da rift (Usuki *et al.* 2015; Tran *et al.* 2015).

The Phan Si Pan zone links two large blocks: North Vietnam – South China block and the Indochina block (Figure 1b), and is located between the Red River Shear Zone and the Tu Le basin. The Phan Si Pan zone is composed of the Mesoarchean-early Paleoproterozoic crystalline basement rocks, which are mainly of biotite quartzite, quartz-biotite-garnet schist, and amphibolite (Minh *et al.* 2021; Pham *et al.* 2022). Palaeo-Mesoproterozoic rocks are biotite schist, two mica schist, and amphibolite (Minh *et al.* 2021; Pham *et al.* 2022). Precambrian magmatism in the area is characterized by (i) Mesoarchean granitoids (2.9–2.8 Ga) (Lan *et al.* 2001; Nam *et al.* 2003; Pham *et al.* 2022); (ii) Paleoproterozoic granitoids (1.8–2.2 Ga) (Nam *et al.* 2003; Zhao *et al.* 2019, 2019b; Pham *et al.* 2022; Zhao *et al.* 2023); (iii) Paleoproterozoic mafic dykes (1.8–2.3 Ga) (Pham *et al.* 2022) and (iv) Neoproterozoic granitoids (760–751 Ma) (Pham *et al.* 2009; Wang *et al.* 2009, 2011, 2016; Minh *et al.* 2021). The Mesoarchean-Paleoproterozoic crystalline basement rocks are unconformably overlain by Palaeozoic-Mesozoic meta-sedimentary and sedimentary rocks, which include quartz-sericite-chlorite schist, quartzite, limestone, and dolomite (Figure 2a,b). In addition to the Precambrian granitoids, during the Late Permian – Early Triassic, voluminous A-type granites are well developed, which are closely related to the Emeishan mantle plume (Pham *et al.* 2013; Tran *et al.* 2015; Usuki *et al.* 2015; Minh *et al.* 2018), and Cenozoic plutons are also recognized in the area (Pham *et al.* 2020; Dung *et al.* 2023). The Neoproterozoic granitoid intrusions mainly include the Posen, Phin Ngan, and Lung Thang plutons together with several small bodies or lenses (Figure 2b) (Li *et al.* 2018). The Neoproterozoic intrusions in the Phan Si Pan zone are well comparable to the equivalents (~860 to ~740 Ma) widely distributed in the west-southwestern Yangtze Block (Figure 1) (Zhou *et al.* Zhou *et al.* 2002; Zhao and Zhou 2008; Cai *et al.* 2014, 2015; Li *et al.* 2018); In this study, representative samples are collected from the Neoproterozoic Lung Thang, Posen and Sin Quyen mine intrusions in northwestern Vietnam (Figure 2b)

3. Sample description

3.1. Lung thang intrusion

The Lung Thang intrusion is located southeast of the Sin Quyen mine (Figure 2b). It intrudes the Paleoproterozoic

meta-sedimentary rocks of the Sin Quyen Formation. The Lung Thang intrusion is composed of medium- to coarse-grained granodiorite with porphyritic-like texture (Figure 3a,b). The dominant minerals are plagioclase (30–50%), K-feldspar (20–30%), quartz (20–30%) and biotite (7–12%), with magnetite, zircon, apatite and titanite as accessory phases (Figure 3a,b). Generally, plagioclase and K-feldspar occur as subhedral to euhedral laths, and some of the grains are coarse (4 to 6 mm) phenocrysts, showing simple lamellar twinning. Quartz occurs as relatively fine, anhedral grains or as interstitial aggregates of small granular grains (Figure 3b). Biotite is anhedral, and pleochroic from yellowish-green to brownish. The weak foliation is defined by the orientation of biotite and feldspar in the groundmass.

3.2. Posen intrusion

The Posen intrusion is characterized by coarse- to medium-grained granodiorite with gneissic structure. The main rock-forming minerals are plagioclase (30–45%), quartz (20–25%), K-feldspar (15–26%), biotite (5–10%) and hornblende (5–15%) (Figure 3c,d). Accessory minerals are titanite, zircon, apatite, magnetite, and epidote. Plagioclase and K-feldspar occur generally as anhedral laths and grains (0.5 to 4 mm). Quartz occurs as deformed, anhedral grains or as interstitial aggregates of small granular grains with weak orientation (Figure 3c). Biotite is anhedral and pleochroic from yellowish-green to brownish. The weak foliation is defined by orientation of biotite, quartz and feldspar (Figure 3d).

3.3. Intrusions in the Sin Quyen mining district

Numerous granitic stocks or dykes intrude Palaeoproterozoic meta-sedimentary rocks, which show different sizes (5–200 m) and shapes, and have undergone through intensive deformation (Li *et al.* 2018). These intrusions are composed of coarse-grained, weakly foliated monzodiorite (Figure 3e,f). The dominant minerals are plagioclase (~48%), biotite (~20%), K-feldspar (~15%), quartz (~8%), and minor amount of hornblende (~9%). Accessory phases are magnetite, zircon and apatite. Plagioclase and K-feldspar occur generally as subhedral to anhedral laths. At places, plagioclase is altered to sericite and/or epidote. Quartz occurs as anhedral grains generally interstitial to feldspar and plagioclase (Figure 3f). Biotite is subhedral to anhedral and flaky with weak orientation (Figure 3e,f). Where present hornblende occurs as subhedral to euhedral prismatic with pleochroism from yellowish-green to deep blue-green.

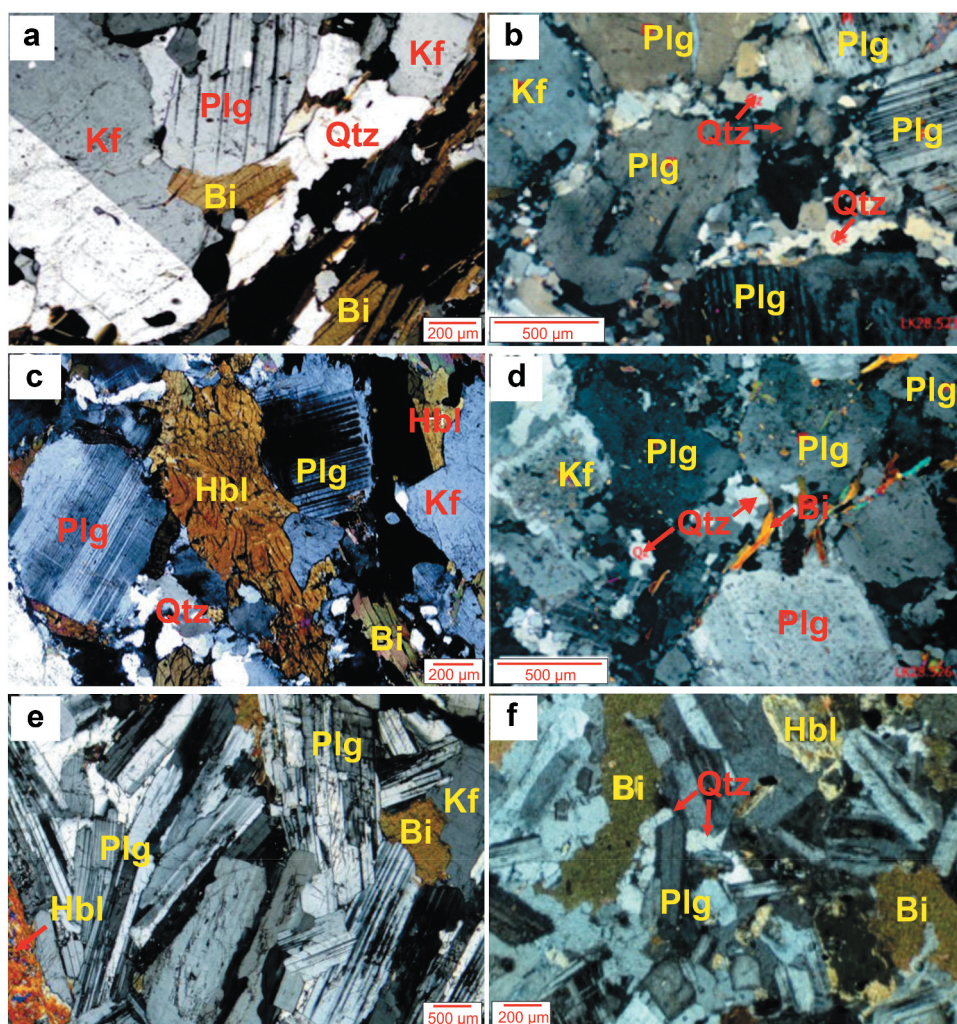


Figure 3. Photomicrographs showing mineral assemblage and texture of (a-b) lung thang, (c-d) Posen and (e-f) sin quyen granitoid. Bi: biotite; Hbl: Hornblend; kf: K-feldspar; plg: plagioclase; and Qtz: quartz.

4. Analytical methods

4.1. LA-ICP-MS zircon U-Pb dating

Magnetic and conventional heavy liquid techniques were used in zircon separation. This process was followed by handpicking under a binocular microscope to separate the zircon grains from fresh granitoid samples. The selected zircons were examined under transmitted and reflected light with an optical microscope, and cathodoluminescence (CL) images were collected on a CAMECA Sx51 under conditions of 50 kV and 15 nA at Wuhan Sample Solution Analytical Technology Co. Ltd. Wuhan, China. The CL images were used to examine the internal textures and to choose potential targets for U–Pb dating and Lu–Hf isotope analysis. U–Pb dating and trace element analyses of separated zircons were conducted in the State Key Laboratory of Geological Processes and Mineral Resources (GPMR), China University of Geosciences

(CUG) Wuhan, China. Experiments were performed on an inductively coupled plasma mass spectrometry (ICPMS; Agilent 7500a Technology, Tokyo, Japan) in combination with an ArF excimer laser ($\lambda = 193$ nm) (GeoLas 2005, MicroLas, Göttingen, Germany). The operating conditions for the LA-ICP-MS instrument were similar to Liu et al (2008, 2010). All analyses were performed with a laser spot size of 32 μm , a repetition rate of 5 Hz, and a fluence of 8 J/cm^2 . Helium was used as a carrier gas in the ablation cell and merged with argon (makeup gas) behind the ablation cell (Günther and Hattendorf 2005; Luo et al. 2018). A signal-smoothing and mercury removing device was used in this laser ablation system to obtain smooth signals and reduce the mercury signal (Hu et al. 2015). A small amount of water vapour (4.1 mg min^{-1}) was added before the ablation cell to improve the analytical accuracy and precision (Luo et al. 2018). Each single-spot analysis consisted of 20 s of background

signal acquisition, followed by 50 s of ablation. Zircon 91,500 (Wiedenbeck *et al.* 1995) was used as an external standard to correct the Pb/U fractionation and instrumental mass discrimination, and zircon GJ-1 was analysed as an unknown. The obtained weighted average $^{206}\text{Pb}/^{238}\text{U}$ ages in 15 analyses of GJ-1 is 598.1 ± 4.1 Ma in this study, which are consistent with the reference age of 599.8 ± 1.7 Ma (Jackson *et al.* 2004). The trace element compositions of zircons were calibrated against NIST 610 glass as an external calibration and combined with ^{29}Si as an internal standardization (Liu *et al.* 2010). Off-line selection and integration of background and analyses signals, and time-drift correction and quantitative calibration for trace element analyses and U-Pb dating were performed by ICPMS Data Cal (Liu *et al.* 2010). Concordia diagrams and weighted mean calculations were made using Isoplot/Ex_ver3 (Ludwig 2003).

4.2. Whole-rock major and trace element analysis

Whole-rock samples were crushed and powdered to 200-mesh in an agate mill. Major element abundances of these samples were obtained by X-ray fluorescence (XRF-1800) at the GPMR, CUG, Wuhan. The accuracy and precision of the XRF data were assessed using Chinese national standards, and duplicate runs on selected samples of the XRF analyses, which are estimated to be $\sim 1\%$ for elements with concentrations >10 wt.% and 5% for the other major elements. More details about the XRF analytical procedure are given by Ma *et al.* (2012) and Wang *et al.* (2013). Whole-rock trace element compositions were determined by an Agilent 7500a ICP-MS, using the techniques described by Liu *et al.* (2008, 2010), and Qi *et al.* (2000). Pure Rb standard solution was used for internal calibration, and GSR-1, BHVO-2, and OU-6 were used as reference materials. The relative errors of the ICP-MS analyses are estimated to be better than ± 5 – 10% for most elements.

4.3. In situ Lu-Hf isotope analysis

In situ Lu-Hf isotope analyses of the dated zircon grains were performed by using Neptune plus multi-collector (MC)-ICPMS system, in combination with a Geolas 2005 system in the GPMR, CUG, Wuhan. The zircons were ablated by a 193 nm ArF Laser system. The spot size of 50 μm was used for analysis, with a laser repetition rate of 10 Hz at 100 mJ/pulse. $^{179}\text{Hf}/^{177}\text{Hf} = 0.7325$ (Chu *et al.* 2002) was used to correct the instrument quality discrimination of Hf isotopes. The instrument quality discrimination factor

for Yb isotopes was calculated using the relationship $\beta_{\text{Yb}} = 0.8725 \times \beta_{\text{Hf}}$ (Xu *et al.* 2004). The correction of ^{176}Hf heterogeneous interference by ^{176}Lu and ^{176}Yb was corrected using $^{176}\text{Yb}/^{172}\text{Yb} = 0.5886$ and $^{176}\text{Lu}/^{175}\text{Lu} = 0.02655$ (Chu *et al.* 2002). The test result of the international standard zircon 91,500 is 0.282301 ± 0.000017 (2σ , $n = 15$), which is consistent with the published value of 0.282307 ± 0.000031 (Wu *et al.* 2006), and of Penglai zircon is 0.282915 ± 0.000014 (2σ , $n = 18$), which is consistent with the published value of 0.282906 ± 0.000010 (Li *et al.* 2010). Additionally, the test result of Plešovice zircon is 0.282477 ± 11 (2σ , $n = 18$), which is consistent with the international recommended value of 0.282482 ± 0.000013 (Sláma *et al.* 2008), and of zircon in Qinghu granite is 0.283002 ± 0.000012 (2σ , $n = 15$), which is consistent with the reported value of 0.283002 ± 0.000004 (Li *et al.* 2013). Calculation methods for $\epsilon_{\text{Hf}}(t)$, T_{DM1} , and T_{DM2} values are similar to those of Wu *et al.* (2008). The detailed analytical procedure followed that described by Yuan *et al.* (2008).

4.4. Whole-rock Sr-Nd isotope analysis

Whole-rock Sr-Nd isotopic compositions were determined using a Finnigan Triton Ti thermal ionization mass spectrometer (TIMS) at GPMR. For details of the analytical procedures, see Wang *et al.* (2013). Powder samples (~ 100 mg) were dissolved in a Teflon bomb with a mixture of concentrated HNO_3 and HF. The samples were dried in an oven at 190°C for 48 h and then converted into chlorides by adding 1 ml of 6 N HCl and dissolved again in 1 ml of 2.5 N HCl. Nd was separated and purified from the final solution using the conventional cation-exchange technique. Mass fractionation for measured Nd isotopic ratios was normalized using a $^{147}\text{Sm}/^{144}\text{Nd}$ ratio of 0.7219. Analyses of standard BCR-2 yielded a mean $^{147}\text{Sm}/^{144}\text{Nd}$ ratio of 0.512655 ± 4 . A ^{47}Sm decay constant (λ) of $6.54 \times 10^{-11} \text{ year}^{-1}$ was adopted for the calculations. We have used the depleted mantle models of Goldstein *et al.* (1984) in our calculations. Fix $\epsilon_{\text{Nd}}(t)$ values were calculated relative to the chondritic uniform reservoir for a present-day $^{147}\text{Sm}/^{144}\text{Nd}$ ratio of 0.512638 and $^{147}\text{Sm}/^{144}\text{Nd}$ ratio of 0.1967. Single-stage (T_{DM1}) Nd model age calculations utilized $^{147}\text{Sm}/^{144}\text{Nd}$ and $^{147}\text{Sm}/^{144}\text{Nd}$ ratios of 0.51315 and 0.2137, respectively, for the present-day depleted mantle.

5. Results

5.1. Zircon morphology and U-Pb ages

Zircon U-Pb data of the studied samples from Lung Thang, Posen and Sin Quyen intrusions are listed in

Supplementary Table S1. Their concordia diagrams and the representative CL images are presented in Figure 4 and Supplementary Figure S1. The CL images show that the majority of zircon grains from Lung Thang, Posen and Sin Quyen have clear oscillatory zoning textures (Supplementary Figure S1) indicating a magmatic origin (Wu and Zheng 2004). Nineteen U-Pb analyses spots on 19 zircon grains from Lung Thang granodiorite have U and Th contents of 106–428 ppm and 57.9–431 ppm with Th/U values of 0.4–1.1, and yield concordant U-Pb ages with a weighted mean $^{206}\text{Pb}/^{238}\text{U}$ age of 803 ± 3 Ma (MSWD = 0.43, 95% confidence interval; Figure 4a). Eighteen U-Pb analyses spots on 18 zircon grains from Posen granodiorite display U contents of 134 to 802 ppm and Th contents of 50 to 538 ppm with Th/U value of 0.08–0.74, suggesting magmatic origin. They have yielded concordant U-Pb ages with a weighted mean $^{206}\text{Pb}/^{238}\text{U}$ age of 777 ± 3 Ma (MSWD = 1.2, 95% confidence interval; Figure 4b). Seventeen U-Pb analyses spots on 17 zircon grains from Sin Quyen monzodiorite have U and Th contents of 99–791 ppm and 37–279 ppm with Th/U value of 0.19–0.93, and yield a concordant U-Pb age with a weighted mean $^{206}\text{Pb}/^{238}\text{U}$ age of 742 ± 3 Ma (MSWD = 1.2, 95% confidence interval; Figure 4c).

5.2. Whole-rock major and trace elements

The Lung Thang and Posen intrusions are granodiorite in composition (Figure 5a,d), characterized by moderate SiO_2 (64.43–65.70 wt.%), with K_2O ranging from 4.05 to 4.89 wt.%, Na_2O varying from 1.68–2.71 wt.%, and CaO varying between 3.99 and 4.72 wt.% (Supplementary Table S2). The Al_2O_3 contents vary from 15.29 to 17.02 wt. %, and A/NK and A/CNK ratios range from 1.72 to 2.11 and 0.94 to 1.03, respectively, suggesting metaluminous to peraluminous compositions (Figure 5b). The $\text{Mg}^\#$ ranges from 45.84 to 46.49. The $\text{Na}_2\text{O} + \text{K}_2\text{O}$ vs. SiO_2 (Figure 5a), and the K_2O vs. SiO_2 (Figure 5c) plots further show all samples belong to subalkaline and high-K calc-alkaline (Arculus 2003), and Cordilleran granitic affinity (Frost *et al.* 2001).

The chondrite-normalized rare-earth element (REE) patterns (Figure 6a) indicate that the Lung Thang and Posen granodiorite show more prominent LREE/HREE fractionation ($\text{LREE}/\text{HREE} = 8.23\text{--}15.71$; and $(\text{La}/\text{Sm})_N = 3.08\text{--}6.02$) with weakly negative Eu anomalies ($\text{Eu}/\text{Eu}^* = 0.87\text{--}0.98$). In the N-MORB-normalized spider diagram (Figure 6g), the rocks are characterized by strong enrichment of large ion lithophile elements (LILE), such as Th, U, K, Rb, La and Ce, and significantly negative anomalies of Nb, Ta, P and Ti.

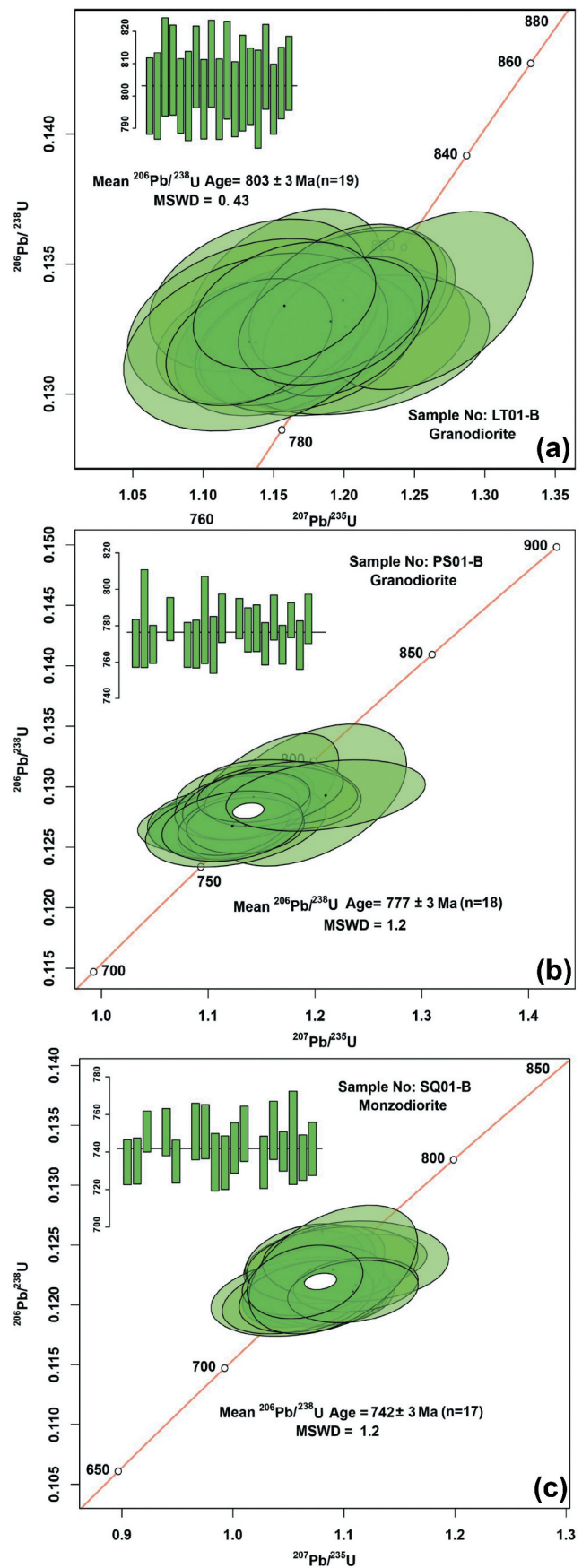


Figure 4. LA-ICP-MS U-Pb concordia diagrams of zircons from (a) lung thang, (b) Posen and (c) Sin Quyen intrusions.

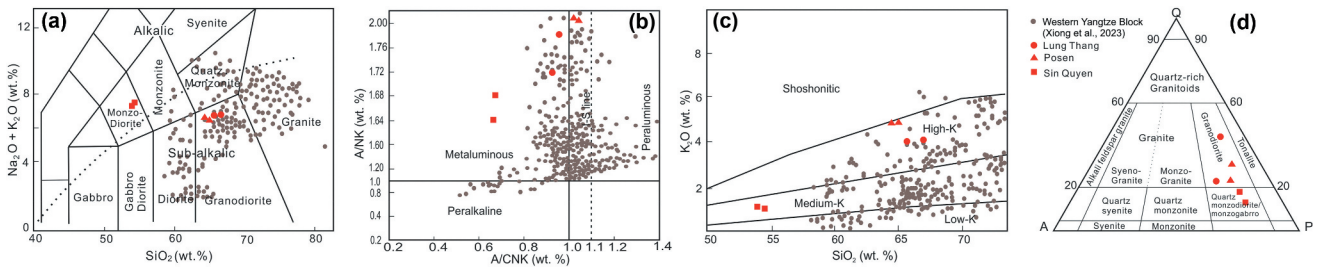


Figure 5. Plots of (a) SiO_2 vs. $(\text{K}_2\text{O} + \text{Na}_2\text{O})$, (b) A/NK vs. A/CNK , (c) K_2O vs. SiO_2 , and (d) QAPF of the studied granitoids. Plots a, b and c are after Middlemost (1994); Frost *et al.* (2001) and Peccerillo and Taylor (1976); respectively.

The Sin Quyen intrusion belongs to monzodiorite in composition (Figure 5a), characterized by medium SiO_2 (53.84–54.20 wt.%), with K_2O ranging from 1.15 to 1.21 wt.%, Na_2O varying from 6.21 to 6.32 wt.%, and CaO varying between 9.35 to 9.41 wt.%, and the Al_2O_3 contents vary from 19.12 to 19.37 wt.% (Supplementary Table S2). The A/NK and A/CNK ratios are 1.64 to 1.68 and 0.67 to 0.68 respectively, suggesting metaluminous composition (Figure 5b). They have low MgO (1.22–1.31 wt.%) with $\text{Mg}^\#$ of 31.32–33.25. On the $\text{Na}_2\text{O} + \text{K}_2\text{O}$ vs. SiO_2 (Figure 5a), and the K_2O vs. SiO_2 (Figure 5c) plots, the Sin Quyen monzodiorites show characteristics of alkaline and medium-K calc-alkaline series (Arculus 2003), and Cordilleran granitic affinity (Frost *et al.* 2001). The chondrite-normalized rare-earth element patterns (Figure 6a) indicate that the Sin Quyen monzodiorite show more prominent LREE/HREE fractionation (LREE/HREE ratios = 4.73–4.76 and $(\text{La}/\text{Sm})_N = 2.69$ –2.73). They show obvious negative Eu anomalies ($\text{Eu}/\text{Eu}^* = 0.63$ –0.64). In the N-MORB-normalized spider diagram (Figure 6g), the Sin Quyen monzodiorites are characterized by enrichment of LILE, such as Th, U, K and Rb, and LREE, including La and Ce, and significantly negative anomalies of Nb, Ta and Ti.

5.3. Zircon Lu-hf isotope compositions

Zircon grains collected from the Lung Thang, Posen and Sin Quyen intrusions that have been used for U-Pb dating were also selected for Lu-Hf isotope analysis. The results are listed in Supplementary Table S3. Ten dated zircon grains from Lung Thang yield $^{176}\text{Hf}/^{177}\text{Hf}$ ratios varying from 0.282061 to 0.282108. Their corresponding $\epsilon_{\text{Hf}}(t)$ values range from -7.9 to -6.1 , yielding a weighted mean value of -6.8 . Single-stage Hf model ages vary from 1.59 to 1.66 Ga, and two-stage Hf model ages range from 2.07 to 2.18 Ga, with a mean T_{DM2} age of 2.12 Ga (Supplementary Table S3). Ten dated zircon grains from Posen intrusion have $^{176}\text{Hf}/^{177}\text{Hf}$ ratios varying from 0.282103 to 0.282174 with $\epsilon_{\text{Hf}}(t)$ values of -4.1 to -6.8 , yielding a weighted mean value of -5.9 . The

single-stage Hf model ages vary from 1.49 to 1.60 Ga, and the two-stage Hf model ages from 1.93 to 2.10 Ga, with a mean T_{DM2} age of 2.03 Ga (Supplementary Table S3). Ten dated zircon grains from the Sin Quyen sample yield $^{176}\text{Hf}/^{177}\text{Hf}$ ratios ranging from 0.28216353 to 0.28253651. Their corresponding $\epsilon_{\text{Hf}}(t)$ values range from -5.8 to $+8.0$, yielding a weighted mean value of $+0.8$. Single-stage Hf model ages range from 0.99 to 1.56 Ga and two-stage Hf model ages range from 1.14 to 2.0 Ga, with a mean T_{DM2} age of 1.60 Ga (Supplementary Table S3).

5.4. Whole-rock Sr-nd isotope compositions

Whole-rock Sr-Nd isotopic compositions of the Lung Thang and Posen granodiorite display $^{143}\text{Nd}/^{144}\text{Nd}$ ratios of 0.511827 to 0.511888 and 0.511927 to 0.511934, corresponding to $\epsilon_{\text{Nd}}(t)$ values of -5.93 to -6.16 and -3.73 to -3.84 at $t = 803$ Ma and 777 Ma, respectively. One-stage depleted-mantle model ages (T_{DM1}) and two-stage depleted-mantle model ages (T_{DM2}) of these samples are 1.9 Ga to 1.6 Ga and 1.8 Ga to 1.6 Ga, respectively (Supplementary Table S4). The Sin Quyen monzodiorite displays $^{143}\text{Nd}/^{144}\text{Nd}$ ratios of 0.512002 to 0.512025, corresponding to $\epsilon_{\text{Nd}}(t)$ values of -5.92 to -6.15 at $t = 742$ Ma (Supplementary Table S4). They yielded one-stage depleted-mantle model ages (T_{DM1}) of 2.12–2.10 Ga and two-stage depleted-mantle model ages (T_{DM2}) of 1.75–1.73 Ga, respectively.

6. Discussion

6.1. Petrogenesis of the intrusions

6.1.1. Lung thang and Posen intrusions

The Lung Thang and Posen intrusions have similar formation time, element geochemical characteristics and Hf-Nd isotope compositions, and therefore they have similar origin. These granitoids show high-K calc-alkaline features. Magmatic rocks of medium- to high-K calc-alkaline composition can be commonly produced

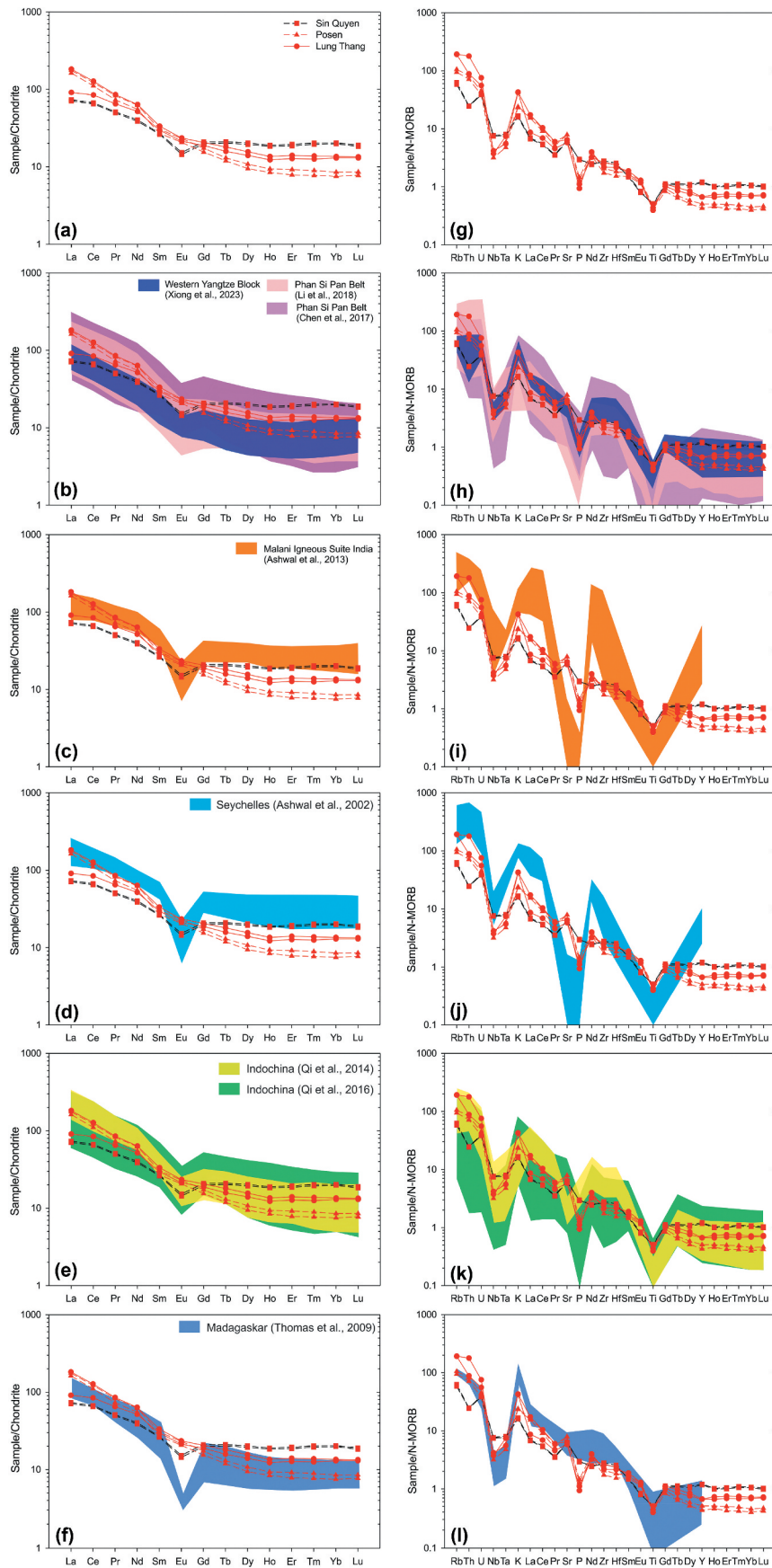


Figure 6. Chondrite-normalized REE and N-MORB-normalized trace element patterns of the Neoproterozoic granitoids. The chondrite and N-MORB values are from Sun and McDonough (1989). Geochemical data of other Neoproterozoic granitoids are for comparison.

by: (1) differentiation of mantle-derived mafic melt (Grove *et al.* 1982; Ewart and Hawkesworth 1987; Be'eri-Shlevin *et al.* 2010; Weissman *et al.* 2013; Khan *et al.* 2021), (2) partial melting of mafic middle-lower crustal rocks due to under-plating of mantle-derived mafic melt (White and Chappell 1983; Beard and Lofgren 1991; Roberts and Clemens 1993; Wolf and Wyllie 1994; Chappell *et al.* 2012; Weissman *et al.* 2013), and (3) mixing of mafic and felsic magmas (DePaolo 1981; Bergantz 1989; Castro *et al.* 1991; Droop *et al.* 2003; Kemp *et al.* 2007; Karsli *et al.* 2010).

In this study, the LA-ICP-MS U-Pb zircon ages of the three representative Neoproterozoic intrusions range from 742 Ma to 803 Ma. These ages are interpreted as the emplacement ages of the Neoproterozoic intrusions in Northwest Vietnam (Supplementary Table S1; Figure 4). Some ~803–814 Ma mafic intrusions have been reported from the Ailaoshan belt (Cai *et al.* 2014), which are the only mantle-derived rocks that could possibly represent the parental magmas of the Lung Thang and Posen intrusions. However, the Lung Thang and Posen intrusions have $\epsilon_{\text{Nd}}(t)$ values (−6.16 to −3.73) clearly lower than those of mafic rocks (−3.5 to +4.4), suggesting that they did not derive from this mafic magma (Figure 7). In addition, the Lung Thang and Posen intrusions display $\epsilon_{\text{Hf}}(t)$ values ranging from −7.9 to −4.1 with $T_{\text{DM}2}$ of 2180–1930 Ma (Supplementary Table S3; Figure 8). Thus, these intrusions should have been mainly derived from partial melting of ancient crustal rocks. Granitoids produced through the mixing of mafic and felsic magmas are normally characterized by the presence of mafic enclaves and a wide range of geochemical compositions. However, no mafic enclaves can be observed in the Lung Thang and Posen intrusions. They also show relatively uniform geochemical composition (Figure 6a,g). These evidences rule out the possibility that the Lung Thang and Posen intrusions were produced by magma mixing.

High and fairly uniform SiO_2 and K_2O , along with low MgO and Fe_2O_3 contents, demonstrate that the Lung Thang and Posen intrusions may have been produced by partial melting of crustal materials at depth, which is further supported their Sr-Nd isotope compositions (Figure 7a). Experimental studies suggest that the content of K_2O in a melt source has a significant influence on the composition of derived melt. For example, meta-tholeiitic rocks have low contents of K_2O , and cannot yield high-K calc-alkaline melts (Roberts and Clemens 1993). In contrast, partial melting of medium- to high-K rocks, such as high-K basalt, can generate a melt with a high K content (Sisson *et al.* 2005). Experimental and geochemical evidence suggests that dehydration melting

of hydrous mineral-bearing mafic rocks under water-undersaturated conditions can generate metaluminous to mildly peraluminous granodioritic melts (Beard and Lofgren 1991; Wolf and Wyllie 1994; Qi *et al.* 2023), whereas water-saturated melting of these rocks commonly generated strong peraluminous melts (Beard and Lofgren 1991; Qi *et al.* 2023). The Lung Thang and Posen intrusions have high K_2O contents and moderate A/CNK values, resembling those of the I-type granitic rocks. Thus, they were probably generated by the dehydration melting of high-K meta-igneous rock at depth. Moreover, the Lung Thang and Posen intrusions have high contents of CaO (3.99–4.72 wt.%), and positive Sr anomalies with little Eu anomalies in the N-MORB-normalized trace element diagram and the chondrite-normalized REE patterns (Figure 6a,g), implying that partial melting occurred at higher pressure (deep level), where minor or no plagioclase was residual in their source; and the produced magma did not undergo marked fractional crystallization of plagioclase. To summarize, the Lung Thang and Posen intrusions were produced by the dehydration melting of ancient, high-K meta-igneous rock at a higher depth.

6.1.2. Sin Quyen intrusion

The Sin Quyen intrusion has high total alkali ($\text{K}_2\text{O}+\text{Na}_2\text{O}=7.36\text{--}7.53$ wt.%), and low MgO (<1.33 wt.%) and Ni (6.55–6.93 ppm), suggesting that its parental magma were mainly from crustal sources. In addition, the $\delta^{18}\text{O}$ values of the intrusion from Sin Quyen mine (7.3–12.4‰; Li *et al.* 2018) are obviously higher than those of typical mantle-derived magmas ($5.3 \pm 0.6\text{‰}$; Valley *et al.* 2005), suggesting the Sin Quyen intrusion was not produced by differentiation of mantle-derived magma.

The magma sources for crustal-derived granitoids include partial melts of igneous or sedimentary rocks in the crust or mixing with mantle-derived melts (Miller 1985; Le Fort *et al.* 1987; Patiño Douce 1999; Zhu *et al.* 2009; Villaseca *et al.* 2012; Maurice *et al.* 2013; Castro 2014). Zircon Hf isotope ratios are not significantly altered by processes of partial melting or fractional crystallization, and therefore indicate open system processes involving more radiogenic (i.e. mantle-derived) and less radiogenic (crustal) end-members (Bolhar *et al.* 2008). The Lu-Hf isotopes act as important geochemical tracers to the melt source (Kemp *et al.* 2006) with distinct characteristics. Melts originating from the residual and depleted mantle or juvenile crust are characterized by high Lu/Hf (i.e. higher than chondritic values) and positive $\epsilon_{\text{Hf}}(t)$ values, whereas melts derived from the ancient crust are characterized by low Lu/Hf (i.e. lower than chondritic values) and negative

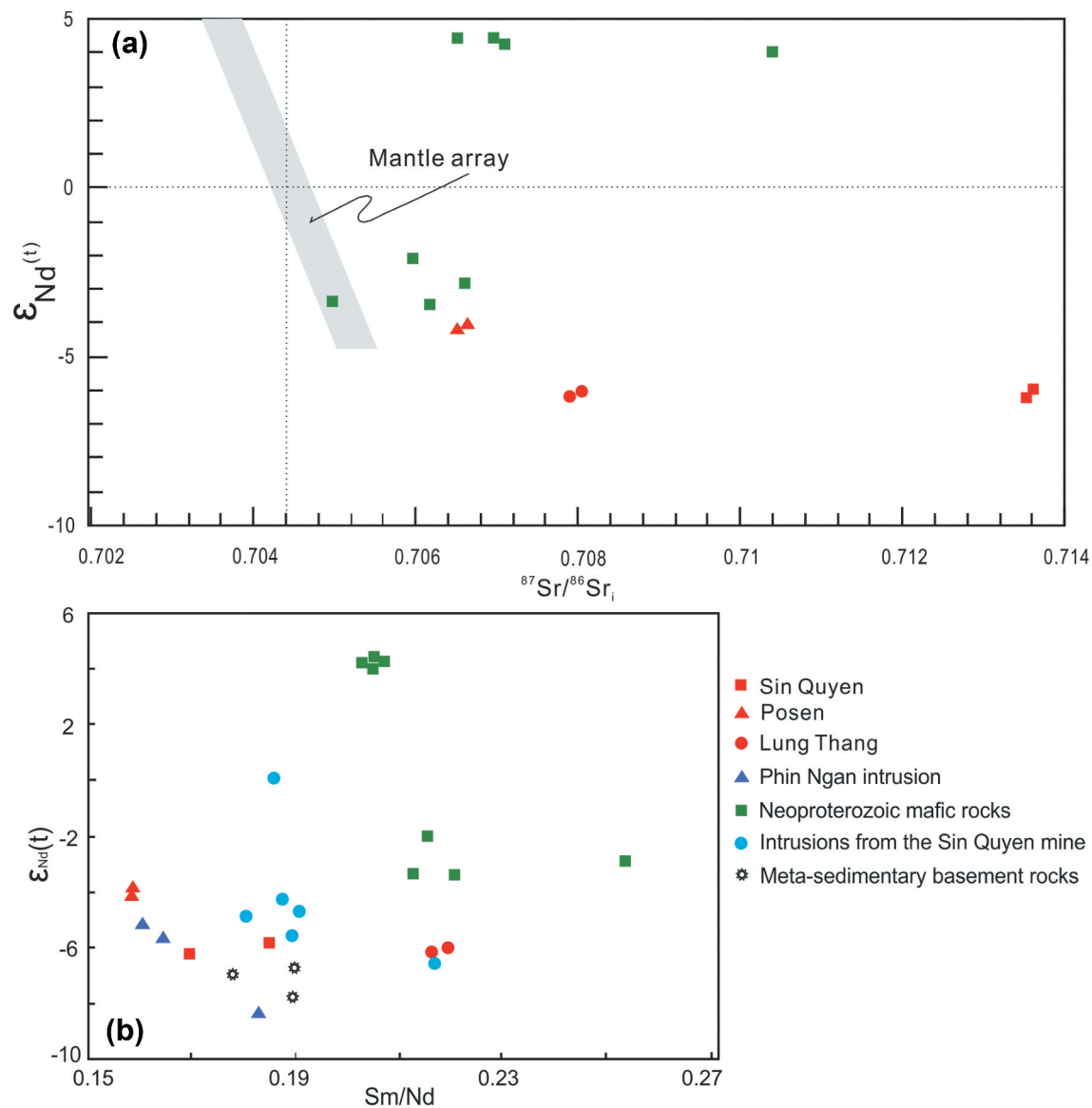


Figure 7. Plot of (a) initial $^{87}\text{Sr}/^{86}\text{Sr}$ vs. $\epsilon_{\text{Nd}}(t)$ and (b) Sm/Nd vs. $\epsilon_{\text{Nd}}(t)$ for the studied granitoids. The data for Phin Ngan, Sin Quyen, meta-sedimentary basement rocks and regional mantle-derived mafic intrusions (from Cai *et al.* 2014; Li *et al.* 2018) are shown for comparison.

$\epsilon_{\text{Hf}}(t)$ values. In addition, a mixed source between the depleted mantle- and ancient crust-derived melts will be characterized by both positive and negative with variable $\epsilon_{\text{Hf}}(t)$ values (Kinny and Maas 2003; Ji *et al.* 2009; Yang *et al.* 2014). The Sin Quyen intrusion show $\epsilon_{\text{Hf}}(t)$ values ranging from -5.8 to $+8$ with T_{DM} of 2013–1143 Ma (Supplementary Table S3; Figure 8), which suggests that the melt for Sin Quyen intrusion might have derived from ancient crustal source mingled with mantle-derived components (Peytcheva *et al.* 2008; Jiang *et al.* 2009; Zhu *et al.* 2009). The Sin Quyen intrusion show sodium-rich with high $\text{Na}_2\text{O}/\text{K}_2\text{O}$ ratios of 5.1–5.5, similar to the normal-arc series rocks (Zhu *et al.* 2017). Experiments have revealed that partial melting of both oceanic and basaltic lower crust

can produce the Na-rich granitic melts (Qian and Hermann 2010, 2013). However, we propose that the mantle-derived endmember is limited due to the consistent values of SiO_2 and $\text{Nd}(t)$ observed in the Sin Quyen intrusion. Therefore, it is suggested that the Sin Quyen intrusion originated mainly from the partial melting of the Mesoproterozoic basaltic lower crust, and mingled with limited mantle-derived magma.

6.2. Tectonic setting

The Lung Thang, Posen and Sin Quyen intrusions are medium- to high-K calc-alkaline in nature, which can

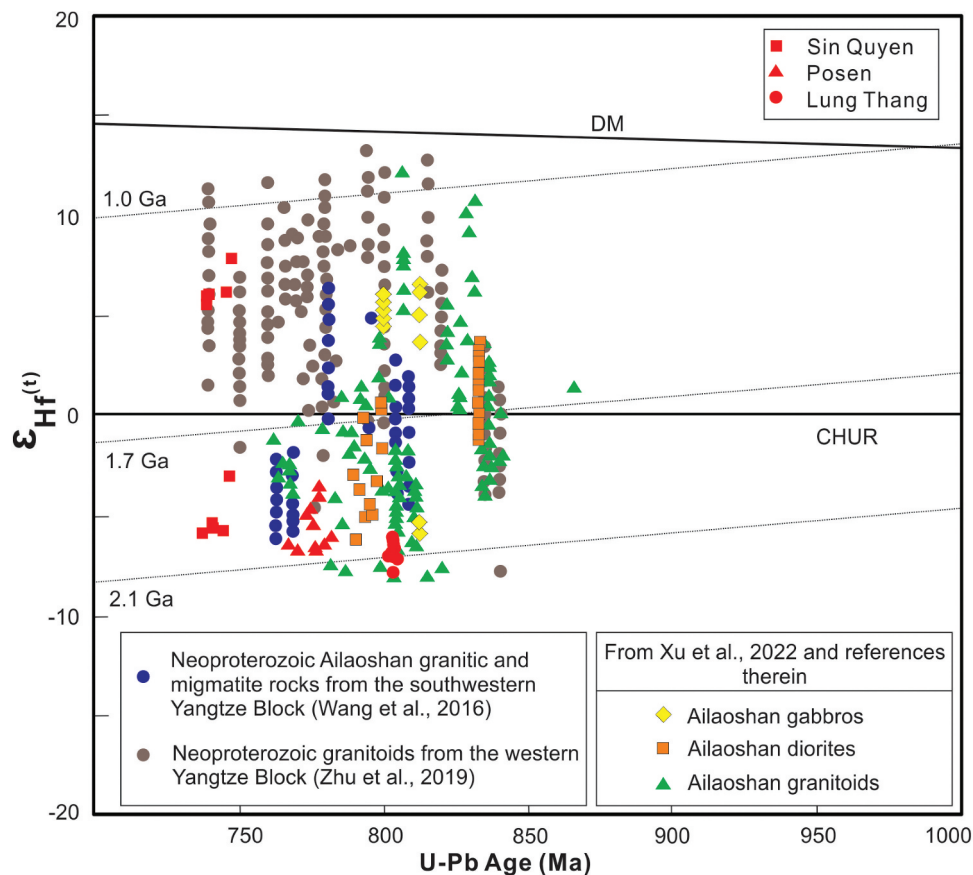


Figure 8. Plot of $\epsilon_{\text{Hf}}(t)$ values versus U-Pb ages of the zircons from the studied granitoids. Zircon Hf isotopic data of Neoproterozoic Ailaoshan granitic and migmatite rocks in the southwestern Yangtze Block are from Wang *et al.* (2016); Zhu *et al.* (2019) and Xu *et al.* (2022). Reference lines representing chondritic uniform reservoir (CHUR) are from Blichert-Toft and Albarede (1997).

be produced in two main tectonic environments. (1) A continental-arc setting (Cordilleran or Andean-type; e.g. Hildreth and Moorbath 1988; Sreejith and Kumar 2013), and (2) syn- to post-collisional settings (Caledonian-type; e.g. Roberts and Clemens 1993). Geochemical data of the Lung Thang, Posen and Sin Quyen intrusions show enrichment of LILE (e.g. Rb, Th and U) and LREE, but depletion of HFSE (e.g. Nb, Ta and Ti). These chemical signatures are typical of calc-alkaline magmatism in active continental margins generated in a subduction-related continental-arc tectonic setting (Sun and McDonough 1989; Hawkesworth *et al.* 1991; Castillo *et al.* 2007). This is well portrayed in the tectonic discrimination diagrams, where the Lung Thang, Posen and Sin Quyen intrusions plot within the field of volcanic arc granitoids (Figure 9). In addition, the Lung Thang and Posen intrusions have geochemical features of adakitic rocks and fall into the adakite and high Si fields (Figure 10), which can compare to adakitic characteristics in west-southwest Yangtze (Zhou *et al.* 2006; Zhao and Zhou 2007; Pham *et al.* 2009; Huang *et al.*

2009). The K-rich adakitic rocks are thought to be formed from magma derived through the partial melting of a thickened region in the lower continental crust, likely linked to orogenesis (Xiao and Clemens 2007; Sheldrick *et al.* 2020). Thus, the Neoproterozoic intrusions of Lung Thang, Posen and Sin Quyen in the Phan Si Pan zone have been proposed to be generated in a subduction-related continental arc setting.

6.3. Tectonic affinity with Yangtze Block and implication for position in Rodinia supercontinent

The tectonic affinity of Northwest Vietnam remains debated. Tectonically, northwestern Vietnam has been linked to either the Indochina (e.g. Qi *et al.* 2012, 2014) or Yangtze blocks (Chung *et al.* 1997; Żelaźniewicz *et al.* 2013). The Neoproterozoic intrusions in Phan Si Pan Zone, northwestern Vietnam (Lung Thang, Posen and Sin Quyen) and Neoproterozoic magmatism in the west-southwestern margin of the South China block (the Panxi-Hannan belt and the Ailaoshan-Red River Shear

zone) (Figure 1) may provide constraints on this issue (Zhou *et al.* 2006; Zhao and Zhou 2007; Pham *et al.* 2009; Huang *et al.* 2009; Cai *et al.* 2014; Qi *et al.* 2014, 2016; Cawood *et al.* 2018; Li *et al.* 2018). Minh *et al.* (2021) reported Neoproterozoic granitoids in the Phan Si Pan Zone (762–758 Ma). Our data identify new Neoproterozoic granitoids in the Phan Si Pan Zone (803–777 Ma and 742 Ma), which are slightly older and younger than their data. Our new geochronological results, along with published data for the Phan Si Pan Zone, have revealed the extensive occurrence of the Neoproterozoic granitic rocks with formation ages ranging from 803 Ma to 742 Ma. These suggest a long-lived Neoproterozoic (803–742 Ma) subduction setting along the Phan Si Pan Zone tectonic zone, which is similar to Neoproterozoic magmatism in the Ailaoshan belt. U-Pb zircon ages (742–803 Ma) of the Neoproterozoic granitoid in Phan Si Pan Zone, northwestern Vietnam in this study are similar to the Neoproterozoic magmatic activities (~740 to ~840 Ma) in the Ailao Shan- Panxi-Hannan belt west-southwestern Yangtze Block (Figure 1b). These age data falls within a prolonged magmatic activity (710 to 870 Ma) along the western-southwestern margin of the Yangtze Block (Zhao and Cawood 2012 and references therein). Some of the Neoproterozoic granitoids in the southwestern Yangtze Block, which are contemporaneous to those of the Phan Si Pan granitoids, such as Jinzhoulin monzogranite (756 ± 9 Ma; Qi *et al.* 2014), Leidashu quartz monzonite (754 ± 4 Ma; Qi *et al.* 2014), Chaojiagou monzogranite (768 ± 11 Ma; Qi *et al.* 2014); Zhetai granite (758 ± 15 Ma; Qi *et al.* 2014), Shayipo granodiorite (765 ± 4 Ma; Qi *et al.* 2016), Datian adakite

(760 ± 4 Ma; Zhao and Zhou 2007) and Gneiss Miyi granitoid (764 ± 9 Ma; Zhou *et al.* 2002). Moreover, isotopic data from the Neoproterozoic rocks in the Phan Si Pan zone are similar in age and characteristics to those in the western-southwestern Yangtze, showing signatures of the volcanic arc setting (Figures 9 and 11). Zircon $\epsilon_{\text{Hf}}(t)$ values (−7.9 to +8.0), $\epsilon_{\text{Nd}}(t)$ values (−6.2 to −3.7) and two-stage Hf model ages ($T_{\text{DM}2} = 1.14\text{--}2.18$ Ma) of the Neoproterozoic rocks in northwestern Vietnam are also consistent with those of the Neoproterozoic rocks in the western-southwestern Yangtze Block (Figure 8; Qi *et al.* 2014, 2016), suggesting similarity of the contemporaneous rocks of the two regions. Recently, Zhao *et al.* (2019, Zhao *et al.* 2019, 2020; Qi *et al.* 2023) proposed that the Phan Si Pan Zone and southwestern Yangtze region experienced similar multi-stage tectono-thermal events during the Archean-Paleoproterozoic period. This finding provides substantial evidence supporting the notion that these two areas share a close tectonic affinity in Precambrian. Additionally, the late Paleoproterozoic sedimentary rocks of both the Phan Si Pan Zone and southwestern Yangtze exhibit similar detrital zircon age patterns. These patterns are marked by prominent age peaks during the Siderian period (2.4–2.2 Ga) and the late Paleoproterozoic era (1.9–1.7 Ga), with minor contributions from the Archean (Zhao *et al.* 2023). Consequently, the magmatic-tectonic record implies that northwest Vietnam is a dismembered part of the western-southwestern Yangtze Block which had been displaced southeastward as a result of the left-lateral Cenozoic movement of the Ailaoshan-Red River fault system (Tapponnier *et al.* 1990).

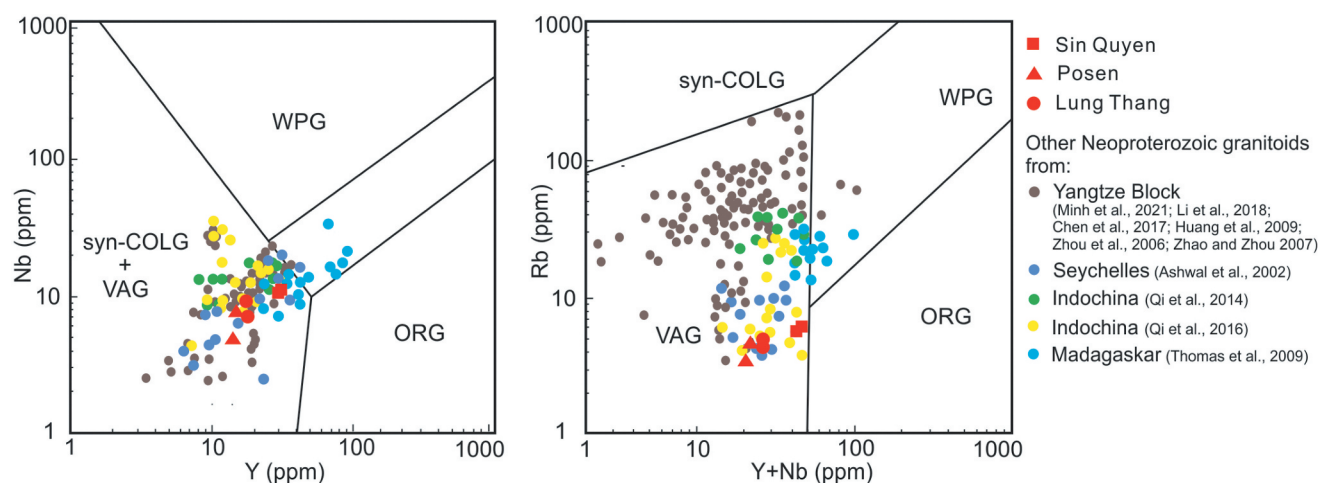


Figure 9. Plot of (a) Y vs. Nb and (b) (Y+nb) vs. Rb for the intrusions in the Ailao Shan-Phan Si Pan belt. The intrusions include Posen granite (Lan *et al.* 2000; Pham *et al.* 2009); Daping granodiorite (Qi *et al.* 2012); Jinzhoulin, Leidashu, Chaojiagou and Zhetai granitoids (Qi *et al.* 2014); Adebo quartz diorite (Cai *et al.* 2015); and lung Thang; Posen; and sin quyen intrusions (this study). Geochemical data of other Neoproterozoic granitoids from Yangtze, Seychelles, Indochina and Madagascar blocks are for comparison. The tectonic classification is from Pearce *et al.* (1984). Syn-COLG = syn-collisional granite; WPG = within plate granite; ORG = orogenic granites; and VAG = volcanic arc granite.

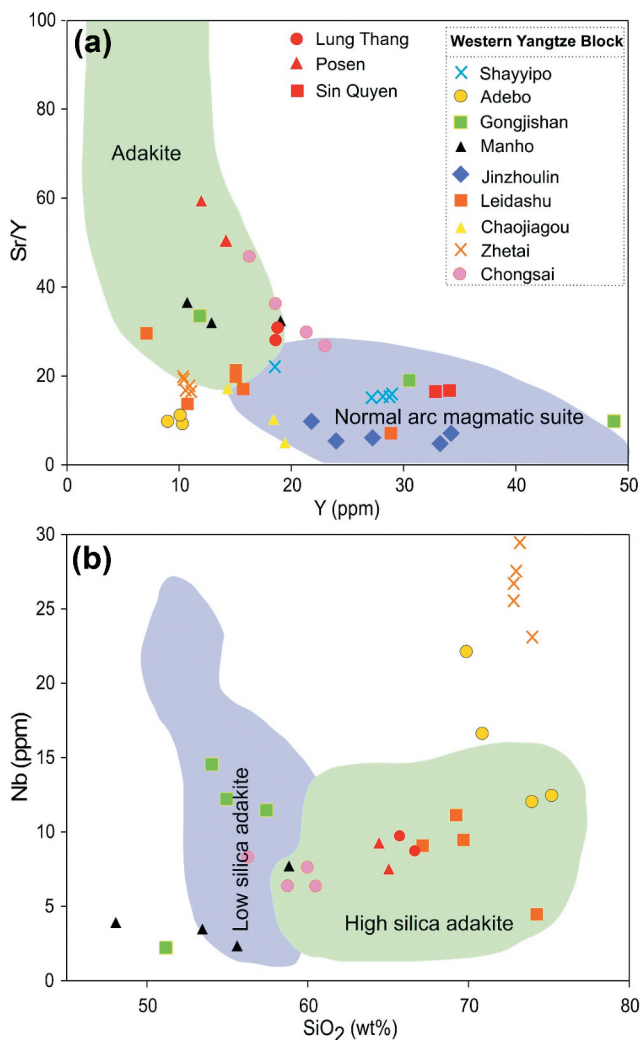


Figure 10. Adakitic diagrams of the studied granitoids (Zhou *et al.* 2006). Geochemical data of other intrusions are from Qi *et al.* (2014, 2016). for comparison.

Neoproterozoic magmatism is widely observed in various continental fragments, such as Australia, Laurentia, South China, India, and Tarim. The occurrence of global Neoproterozoic magmatism is often associated with mantle plumes or a mantle super-plume, which led to the rifting and eventual break-up of the Neoproterozoic Rodinia supercontinent (Li *et al.* 2002; Wang *et al.* 2009; Ernst *et al.* 2016; Likhanov and Santosh 2017). However, some studies suggest that the Neoproterozoic magmatism found in the Seychelles, Madagascar, and Greater India was formed within a giant continuous continental arc, indicating the presence of an active Andean-type orogeny along the northwestern periphery of the Rodinia supercontinent (Gregory *et al.* 2009; Ding and Zhang 2016). The position of the South China Block has been suggested to be either between Australia and Laurentia (Li *et al.* 2002)

or connected to India within the Rodinia supercontinent (Yu *et al.* 2008).

The widespread Neoproterozoic magmatism along the western and southwestern margin of the Yangtze Block has been attributed to subduction of oceanic lithosphere underneath the Yangtze Block (Zhou *et al.* 2006; Qi *et al.* 2014, 2016; Cawood *et al.* 2018). Geochemical features of the Lung Thang, Posen and Sin Quyen intrusions are enrichment of LILE (e.g. Rb, Th and U) and LREE, depletion of HFSE (e.g. Nb, Ta and Ti), and plot in the field of volcanic arc granitoids (Figure 9). They also have geochemical features of adakitic rocks and fall into the adakite and high Si fields (Figure 10), which can compare to adakitic characteristics in west-southwest Yangtze (Zhou *et al.* 2006; Zhao and Zhou 2007; Pham *et al.* 2009; Huang *et al.* 2009). The Neoproterozoic granitoids in the Ailao Shan-Phan Si Pan belt also show similar geochemical features in a subduction-related setting (Qi *et al.* 2012, 2014; Cai *et al.* 2014, 2015; Wang *et al.* 2016; Li *et al.* 2018). Contemporary Nb-enriched and arc-like metabasite (750–800 Ma) were also reported in the the Ailaoshan area (Cai *et al.* 2014, 2015). Moreover, the Neoproterozoic granitoids in the Phan Si Pan Zone show similar zircon Hf isotopes to Neoproterozoic granitoids from the Ailao Shan belt (Wang *et al.* 2016), suggesting they have a similar origin. However, Neoproterozoic granitoids in the Phan Si Pan Zone show different zircon Hf isotopes from those in the western Yangtze (Panxi-Hannan arc system) (Figure 8), indicating different origins. Wang *et al.* (2016) suggest the presence of a Neoproterozoic convergent environment around the Yangtze Block, from Ailaoshan to Panxi, and then to Hannan. Thus, the different zircon Hf isotopes between the Hannan-Panxi belt and Ailaoshan-Phan Si Pan belt may suggest that the basement of these two regions is distinct. The Neoproterozoic intrusions of Lung Thang, Posen and Sin Quyen in the Phan Si Pan zone have been proposed to be generated in a subduction-related setting. The development of such long-lived Neoproterozoic magmatism is much later than the global Grenvillian (ca. 1.0–1.3 Ga) orogeny along Laurentia, Australia and East Antarctica (Cawood *et al.* 2010; 2013), suggesting the Yangtze Block located on the periphery rather than in the intracraton of Rodinia. Therefore, we propose South China Block (including Northwest Vietnam) on the periphery of the Neoproterozoic Rodinia supercontinent.

The extensive magmatic rocks from the northwestern margin of the Greater India, the northeastern margin of Indochina Block and SW Yangtze Block, Lhasa and the Phan Si Pan zone in northwest Vietnam (Hill and Walter 2000; Li *et al.* 2006; Piper 2007; Thomas *et al.* 2009; Van Lente *et al.* 2009; Santosh *et al.* 2012; Ashwal *et al.* 2013;

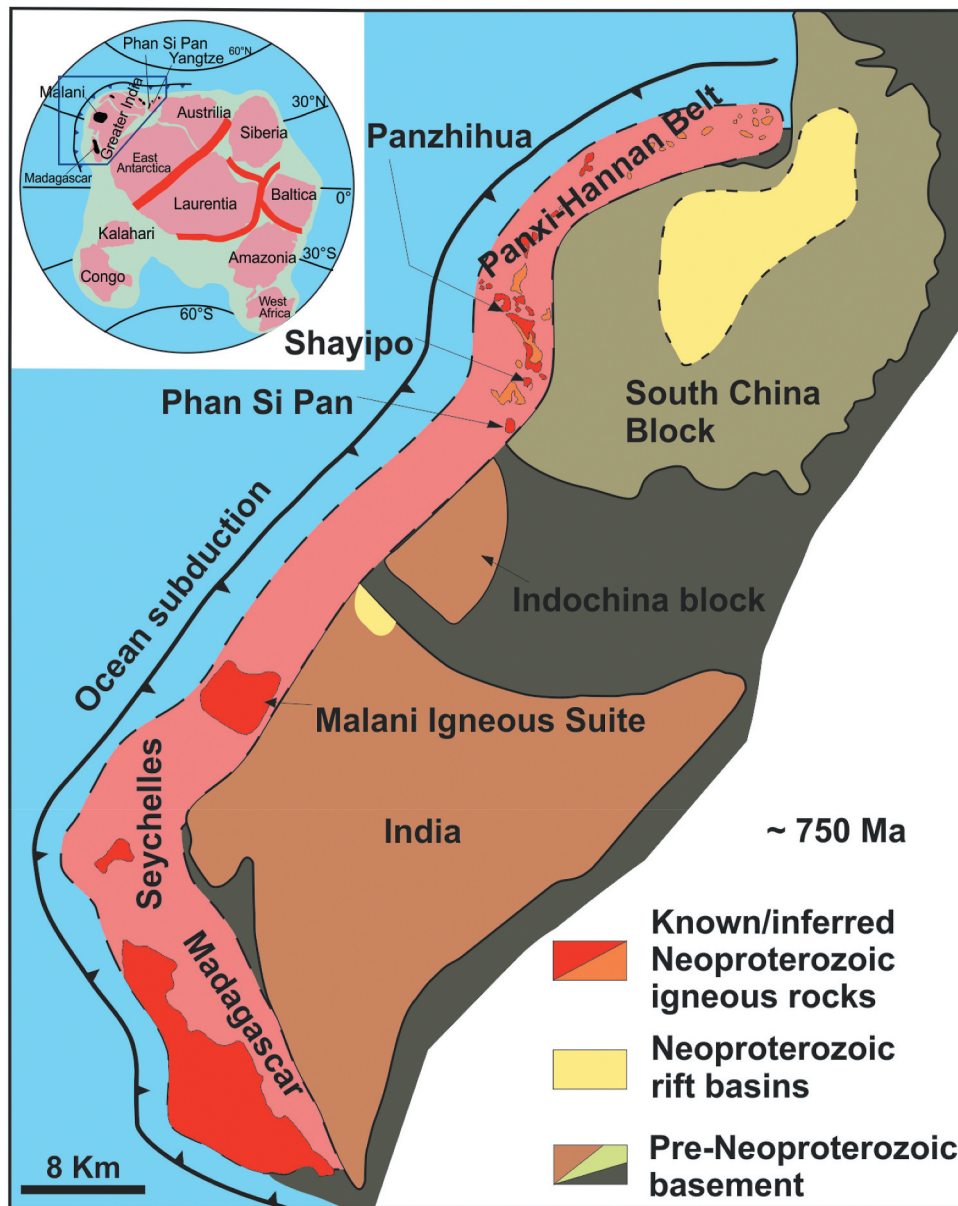


Figure 11. Paleogeographic reconstruction depicting juxtaposition of South China and Indochina blocks with greater India, the Seychelles and Madagascar defining a Neoproterozoic (~750 ma) giant magmatic belt against an eastward subducting ocean (Zhou *et al.* 2006; Cawood *et al.* 2018).

Dharma Rao *et al.* 2013; Santosh *et al.* 2015; Cawood *et al.* 2018; Qi *et al.* 2014, 2016; Cai *et al.* 2014; Zhu *et al.* 2019 and references therein) exhibit similar geochemical characteristics, such as fractionated rare earth element (REE) patterns with negative anomalies for Nb, Ta, and Ti (Figure 6), further supporting their affinity to arc-related magmatism. Based on a comprehensive analysis of the geochemical and geochronological data from previous research, as well as data presented in this work (Figures 6 and 7), we propose that the Greater India, Lhasa, Indochina, Seychelles, Madagascar, Yangtze were situated along the western and northern margins of the Rodinia supercontinent (Figure 11). These blocks

experienced a shared Neoproterozoic magmatic event on the northwestern margin of the Rodinia supercontinent. This Neoproterozoic magmatic event affected the aforementioned regions and was a result of the tectonic processes associated with the Andean-type orogeny. These processes typically involve the subduction of oceanic crust beneath a continental plate, leading to the formation of arc-related magmatism. It is worth noting that the concept of the Rodinia supercontinent and its exact configuration during the Neoproterozoic is still a subject of scientific investigation and ongoing research. However, based on current understanding, the proposed link between the

mentioned regions and the Neoproterozoic magmatic event associated with the Andean-type orogeny on the northwestern margin of Rodinia provides a plausible explanation for the geological history of these areas.

6. Conclusions

The Lung Thang, Posen and Sin Quyen intrusions in the Phan Si Pan zone, northwest Vietnam show medium- to high-K calc-alkaline affinity. The LA-ICP-MS U-Pb dating of zircons from intrusions of the Phan Si Pan zone, northwest Vietnam yields Neoproterozoic emplacement ages of 803 Ma for Lung Thang, 777 Ma for Posen and 742 Ma for Sin Quyen. The Lung Thang, Posen and Sin Quyen intrusions show medium- to high-K calc-alkaline affinity. These intrusions are characterized by the enrichment of LILE (Th, U, K, Rb) and LREE, and strong negative anomalies of Nb, Ta, and Ti, suggesting their formation in a subduction-related tectonic environment. Whole-rock $\epsilon_{\text{Nd}}(t)$ (−6.16 to −3.73) and zircon $\epsilon_{\text{Hf}}(t)$ values (−7.9 to −4.1 with $T_{\text{DM}2}$ of 2180–1930 Ma), and high-K character of the Lung Thang and Posen intrusions suggest that these intrusions were generated by partial melting of ancient, high-K meta-igneous rock at a higher depth. However, whole-rock $\epsilon_{\text{Nd}}(t)$ (−6.15 to −5.92) and zircon $\epsilon_{\text{Hf}}(t)$ (−5.8 to +8 with T_{DM} of 2013–1143 Ma) values of the Sin Quyen intrusion suggest its generation from a melt produced by partial melting of Mesoproterozoic basaltic lower crust mingled with limited mantle-derived components. The ages, geochemical characteristics, and tectonic settings of these intrusions are similar to those occurring in the Ailaoshan belt along the southwestern margin of the Yangtze block in South China, northeast of Indochina block and northwestern margin of Greater India as well as those in Seychelles and northern Madagascar, suggesting a similar history and synchronous episode of crustal growth/recycling in an Andean-type arc system along the western margin of the Rodinia supercontinent during the Neoproterozoic and juxtaposition of these blocks.

Disclosure statement

No potential conflict of interest was reported by the author(s).

Funding

The work was supported by the Vietnam Ministry of Education and Training [B2022-MDA-15].

References

- Anh, T.V., Pang, K.N., Chung, S.L., Lin, H.M., Hoa, T.T., Anh, T.T., and Yang, H.J., 2011, The Song Da magmatic suite revisited: A petrologic, geochemical and Sr–Nd isotopic study on picrites, flood basalts and silicic volcanic rocks: *Journal of Asian Earth Sciences*, v. 42, no. 6, p. 1341–1355. [10.1016/j.jseaes.2011.07.020](https://doi.org/10.1016/j.jseaes.2011.07.020)
- Ao, W., Zhao, Y., Zhang, Y., Zhai, M., Zhang, H., Zhang, R., Wang, Q., and Sun, Y., 2019, The Neoproterozoic magmatism in the northern margin of the Yangtze Block: Insights from Neoproterozoic (950–706 ma) gabbroic–granitoid rocks of the Hannan complex: *Precambrian Research*, v. 333, p. 105442. [10.1016/j.precamres.2019.105442](https://doi.org/10.1016/j.precamres.2019.105442)
- Arculus, R.J., 2003, Use and abuse of the terms calcalkaline and calcalkalic: *Journal of Petrology*, v. 44, no. 5, p. 929–935. [10.1093/petrology/44.5.929](https://doi.org/10.1093/petrology/44.5.929)
- Ashwal, L., Demaiffe, D., and Torsvik, T., 2002, Petrogenesis of neoproterozoic granitoids and related rocks from the Seychelles: The case for an Andean-type arc origin: *Journal of Petrology*, v. 43, no. 1, p. 45–83. [10.1093/petrology/43.1.45](https://doi.org/10.1093/petrology/43.1.45)
- Ashwal, L., Solanki, A., Pandit, M., Corfu, F., Hendriks, B., Burke, K., and Torsvik, T., 2013, Geochronology and geochemistry of neoproterozoic Mt. Abu granitoids, NW India: Regional correlation and implications for Rodinia paleogeography: *Precambrian Research*, v. 236, p. 265–281. [10.1016/j.precamres.2013.07.018](https://doi.org/10.1016/j.precamres.2013.07.018)
- Baig, S.S., Xue, C., Jan, M.Q., and Rehman, H.U., 2021, Late Jurassic adakite-like granodiorite along the southern Karakoram block, NE Pakistan: New evidence for subduction initiation of the Neo-Tethys Ocean: *Lithos*, v. 406–407, p. 106496.
- Beard, J.S., and Lofgren, G.E., 1991, Dehydration melting and water-saturated melting of basaltic and andesitic greenstones and amphibolites at 1, 3, and 6. 9 kb: *Journal of Petrology*, v. 32, no. 2, p. 365–401. [10.1093/petrology/32.2.365](https://doi.org/10.1093/petrology/32.2.365)
- Be'eri-Shlevin, Y., Katzir, Y., Blichert-Toft, J., Kleinhanns, I.C., and Whitehouse, M.J., 2010, Nd–Sr–Hf–O isotope provinciality in the northernmost Arabian–Nubian shield: Implications for crustal evolution: *Contributions to Mineralogy and Petrology*, v. 160, no. 2, p. 181–201. [10.1007/s00410-009-0472-8](https://doi.org/10.1007/s00410-009-0472-8)
- Bergantz, G.W., 1989, Underplating and partial melting: Implications for melt generation and extraction: *Science*, v. 245, no. 4922, p. 1093–1095. [10.1126/science.245.4922.1093](https://doi.org/10.1126/science.245.4922.1093)
- Blichert-Toft, J., and Albarede, F., 1997, The Lu–Hf isotope geochemistry of chondrites and the evolution of the mantle–crust system: *Earth and Planetary Science Letters*, v. 148, no. 1–2, p. 243–258. [10.1016/S0012-821X\(97\)00040-X](https://doi.org/10.1016/S0012-821X(97)00040-X)
- Boger, S.D., 2011, Antarctica — before and after Gondwana: *Gondwana Research*, v. 19, no. 2, p. 335–371. [10.1016/j.gr.2010.09.003](https://doi.org/10.1016/j.gr.2010.09.003)
- Bolhar, R., Weaver, S.D., Whitehouse, M.J., Palin, J.M., Woodhead, J.D., and Cole, J.W., 2008, Sources and evolution of arc magmas inferred from coupled O and Hf isotope systematics of plutonic zircons from the Cretaceous separation point suite (New Zealand): *Earth and Planetary Science Letters*, v. 268, no. 3, p. 312–324. [10.1016/j.epsl.2008.01.022](https://doi.org/10.1016/j.epsl.2008.01.022)
- Cai, Y., Wang, Y., Cawood, P.A., Fan, W., Liu, H., Xing, X., and Zhang, Y., 2014, Neoproterozoic subduction along the Ailaoshan zone, South China: Geochronological and

- geochemical evidence from amphibolite: *Precambrian Research*, v. 245, p. 13–28. [10.1016/j.precamres.2014.01.009](https://doi.org/10.1016/j.precamres.2014.01.009)
- Cai, Y., Wang, Y., Cawood, P.A., Zhang, Y., and Zhang, A., 2015, Neoproterozoic crustal growth of the Southern Yangtze Block: Geochemical and zircon U–pb geochronological and Lu–hf isotopic evidence of neoproterozoic diorite from the Ailaoshan zone: *Precambrian Research*, v. 266, p. 137–149. [10.1016/j.precamres.2015.05.008](https://doi.org/10.1016/j.precamres.2015.05.008)
- Castillo, P.R., Rigby, S.J., and Solidum, R.U., 2007, Origin of high field strength element enrichment in volcanic arcs: Geochemical evidence from the sulu arc, southern Philippines: *Lithos*, v. 97, no. 3–4, p. 271–288. [10.1016/j.lithos.2006.12.012](https://doi.org/10.1016/j.lithos.2006.12.012)
- Castro, A., 2014, The off-crust origin of granite batholiths: *Geoscience Frontiers*, v. 5, no. 1, p. 63–75. [10.1016/j.gsf.2013.06.006](https://doi.org/10.1016/j.gsf.2013.06.006)
- Castro, A., Moreno-Ventas, I., and de la Rosa, J.D., 1991, H-type (hybrid) granitoids: A proposed revision of the granite-type classification and nomenclature: *Earth Science Review*, v. 31, no. 3, p. 237–253. [10.1016/0012-8252\(91\)90020-G](https://doi.org/10.1016/0012-8252(91)90020-G)
- Cawood, P.A., Strachan, R., Cutts, K., Kinny, P.D., Hand, M., and Pisarevsky, S., 2010, Neoproterozoic orogeny along the margin of Rodinia: Valhalla orogen: *North Atlantic Geology*, 38, no. 2.
- Cawood, P.A., Wang, Y.J., Xu, Y.J., and Zhao, G.C., 2013, Locating South China in Rodinia and Gondwana: A fragment of greater India lithosphere?: *Geology*. [10.1130/G34395.1](https://doi.org/10.1130/G34395.1)
- Cawood, P.A., Wang, W., Zhao, T., Xu, Y., Mulder, J.A., Pisarevsky, S.A., Zhang, L., Gan, C., He, H., Liu, H., Qi, L., Wang, Y., Yao, J., Zhao, G., Zhou, M.F., and Zi, J.W., 2020, Deconstructing South China and consequences for reconstructing Nuna and Rodinia: *Earth-Science Reviews*, v. 204, p. 103169. [10.1016/j.earscirev.2020.103169](https://doi.org/10.1016/j.earscirev.2020.103169)
- Cawood, P.A., Zhao, G., Yao, J., Wang, W., Xu, Y., and Wang, Y., 2018, Reconstructing South China in Phanerozoic and Precambrian supercontinents: *Earth Science Review*, v. 186, p. 173–194. [10.1016/j.earscirev.2017.06.001](https://doi.org/10.1016/j.earscirev.2017.06.001)
- Chappell, B.W., Bryant, C.J., and Wyborn, D., 2012, Peraluminous I-type granites: *Lithos*, v. 153, p. 142–153. [10.1016/j.lithos.2012.07.008](https://doi.org/10.1016/j.lithos.2012.07.008)
- Chen, X., Liu, J., Fan, W., Qi, Y., Wang, W., Chen, J., and Burg, J.P., 2017, Neoproterozoic granitoids along the Ailao Shan-Red River belt: Zircon U–Pb geochronology, Hf isotope analysis and tectonic implications: *Precambrian Research*, v. 299, p. 244–263.
- Chung, S.-L., Lee, T.-Y., Lo, C.-H., Wang, P.-L., Chen, C.-Y., Yem, N. T., Hoa, T.T., and Genyao, W., 1997, Intraplate extension prior to continental extrusion along the Ailao Shan-Red River shear zone: *Geology*, v. 25, no. 4, p. 311–314. [10.1130/0091-7613\(1997\)025<0311:IEPTCE>2.3.CO;2](https://doi.org/10.1130/0091-7613(1997)025<0311:IEPTCE>2.3.CO;2)
- Chu, N.-C., Taylor, R.N., Chavagnac, V., Nesbitt, R.W., Boella, R.M., Milton, J.A., German, C.R., Bayon, G., and Burton, K., 2002, Hf isotope ratio analysis using multi-collector inductively coupled plasma mass spectrometry: An evaluation of isobaric interference corrections: *Journal of Analytical Atomic Spectrometry*, v. 17, no. 12, p. 1567–1574. [10.1039/b206707b](https://doi.org/10.1039/b206707b)
- DePaolo, D.J., 1981, A neodymium and strontium isotopic study of the Mesozoic calc-alkaline granitic batholiths of the Sierra Nevada and Peninsular Ranges: *California: Journal of Geophysical Research: Solid Earth*, v. 86, no. B11, p. 10470–10488. [10.1029/JB086iB11p10470](https://doi.org/10.1029/JB086iB11p10470)
- DGMVN (Department of Geology and Minerals of Vietnam), 1995, *Geology of Vietnam: Stratigraphy*: Hanoi: Science Publisher, v. 1, p. 1–359. (in Vietnamese).
- Dharma Rao, C.V., Santosh, M., Kim, S.W., and Li, S., 2013, Arc magmatism in the Delhi Fold Belt: SHRIMP U–Pb zircon ages of granitoids and implications for Neoproterozoic convergent margin tectonics in NW India: *Journal of Asian Earth Sciences*, v. 78, p. 83–99. [10.1016/j.jseaes.2012.09.007](https://doi.org/10.1016/j.jseaes.2012.09.007)
- Ding, H., and Zhang, Z., 2016, Neoproterozoic granitoids in the eastern Himalayan orogen and their tectonic implications: *Precambrian Research*, v. 285, p. 1–9. [10.1016/j.precamres.2016.09.005](https://doi.org/10.1016/j.precamres.2016.09.005)
- Droop, G., Clemens, J., and Dalrymple, D., 2003, Processes and conditions during contact anatexis, melt escape and restite formation: The Huntly gabbro complex: NE Scotland: *Journal of Petrology*, v. 44, no. 6, p. 995–1029. [10.1093/petrology/44.6.995](https://doi.org/10.1093/petrology/44.6.995)
- Dung, P.T., Usuki, T., Tran, H.T., Tran, H.T., Hoang, N., Usuki, M., Minh, P., Nong, A.T.Q., Nguyen, Y.V., and Pham, T.H., 2023, Emplacement ages, geochemical and Sr–nd–hf isotopic characteristics of Cenozoic granites in the Phan Si Pan uplift, Northwestern Vietnam: Petrogenesis and tectonic implication for the adjacent structure of the red river shear zone: *International Journal of Earth Sciences (Geol Rundsch)*, v. 112, p. 1475–1497. [10.1007/s00531-023-02307-4](https://doi.org/10.1007/s00531-023-02307-4)
- Ernst, R.E., Hamilton, M.A., Söderlund, U., Hanes, J.A., Gladkochub, D.P., Okrugin, A.V., Kolotilina, T., Mekhonoshin, A.S., Bleeker, W., Lecheminant, A.N., Buchan, K.L., Chamberlain, K.R., and Didenko, A.N., 2016, Long-lived connection between southern Siberia and northern Laurentia in the proterozoic: *Nature Geoscience*, v. 9, no. 6, p. 464–469. [10.1038/ngeo2700](https://doi.org/10.1038/ngeo2700)
- Ewart, A., and Hawkesworth, C.J., 1987, The Pleistocene-recent Tonga-kermadec arc lavas: Interpretation of new isotopic and rare earth data in terms of a depleted mantle source model: *Journal of Petrology*, v. 28, no. 3, p. 495–530. [10.1093/petrology/28.3.495](https://doi.org/10.1093/petrology/28.3.495)
- Faisal, S., Larson, K.P., King, J., and Cottle, J.M., 2016, Rifting, subduction and collisional records from pluton petrogenesis and geochronology in the Hindu Kush: NW Pakistan: *Gondwana Research*, v. 35, p. 286–304. [10.1016/j.gr.2015.05.014](https://doi.org/10.1016/j.gr.2015.05.014)
- Faure, M., Lepvrier, C., Van Nguyen, V., Van Vu, T., Lin, W., and Chen, Z., 2014, The South China block-Indochina collision: Where, when, and how?: *Journal of Asian Earth Sciences*, v. 79, p. 260–274. [10.1016/j.jseaes.2013.09.022](https://doi.org/10.1016/j.jseaes.2013.09.022)
- Faure, M., Lin, W., Chu, Y., and Lepvrier, C., 2016, Triassic tectonics of the southern margin of the South China block: *Comptes Rendus Geoscience*, v. 348, no. 1, p. 5–14. [10.1016/j.crte.2015.06.012](https://doi.org/10.1016/j.crte.2015.06.012)
- Frost, B.R., Barnes, C.G., Collins, W.J., Arculus, R.J., Ellis, D.J., and Frost, C.D., 2001, A geochemical classification for granitic rocks: *Journal of Petrology*, v. 42, no. 11, p. 2033–2048. [10.1093/petrology/42.11.2033](https://doi.org/10.1093/petrology/42.11.2033)
- Goldstein, S.L., O’Nions, R.K., and Hamilton, P.J., 1984, A Sm–nd isotopic study of atmospheric dusts and particulates from major river systems: *Earth and Planetary Science Letters*, v. 70, no. 2, p. 221–236. [10.1016/0012-821X\(84\)90007-4](https://doi.org/10.1016/0012-821X(84)90007-4)
- Gregory, L.C., Meert, J.G., Bingen, B., Pnadt, M.K., and Torsvik, T. H., 2009, Paleomagnetism and geochronology of the Malani igneous suite, Northwest India: Implications for the configuration of Rodinia and the assemblage of Gondwana:

- Precambrian Research, v. 170, p. 13–26. [10.1016/j.precamres.2008.11.004](https://doi.org/10.1016/j.precamres.2008.11.004)
- Grove, T.L., Gerlach, D.C., and Sando, T.W., 1982, Origin of calc-alkaline series lavas at Medicine Lake volcano by fractionation, assimilation and mixing: Contributions to Mineralogy and Petrology, v. 80, no. 2, p. 160–182. [10.1007/BF00374893](https://doi.org/10.1007/BF00374893)
- Günther, D., and Hattendorf, B., 2005, Solid sample analysis using laser ablation inductively coupled plasma mass spectrometry: TrAC Trends in Analytical Chemistry, v. 24, no. 3, p. 255–265. [10.1016/j.trac.2004.11.017](https://doi.org/10.1016/j.trac.2004.11.017)
- Hawkesworth, C.J., Hergt, J.M., McDermott, F., and Ellam, R.M., 1991, Destructive margin magmatism and the contributions from the mantle wedge and subducted crust: Australian Journal of Earth Sciences, v. 38, no. 5, p. 577–594. [10.1080/08120099108727993](https://doi.org/10.1080/08120099108727993)
- Hildreth, W., and Moorbath, S., 1988, Crustal contributions to arc magmatism in the Andes of central Chile: Contributions to Mineralogy and Petrology, v. 98, no. 4, p. 455–489. [10.1007/BF00372365](https://doi.org/10.1007/BF00372365)
- Hill, A.C., and Walter, M.R., 2000, Mid-neoproterozoic (~830–750 ma) isotope stratigraphy of Australia and global correlation: Precambrian Research, v. 100, no. 1, p. 181–211. [10.1016/S0301-9268\(99\)00074-1](https://doi.org/10.1016/S0301-9268(99)00074-1)
- Huang, X.-L., Xu, Y.-G., Lan, J.-B., Yang, Q.-J., and Luo, Z.-Y., 2009, Neoproterozoic adakitic rocks from mopanshan in the western Yangtze Craton: Partial melts of a thickened lower crust: Lithos, v. 112, no. 3–4, p. 367–381. [10.1016/j.lithos.2009.03.028](https://doi.org/10.1016/j.lithos.2009.03.028)
- Hu, Z., Zhang, W., Liu, Y., Gao, S., Li, M., Zong, K., Chen, H., and Hu, S., 2015, Wave signal-smoothing and mercury-removing device for laser ablation quadrupole and multiple collector ICPMS analysis: Application to lead isotope analysis: Analytical Chemistry, v. 87, no. 2, p. 1152–1157. [10.1021/ac503749k](https://doi.org/10.1021/ac503749k)
- Jackson, S.E., Pearson, N.J., Griffin, W.L., and Belousova, E.A., 2004, The application of laser ablation-inductively coupled plasma-mass spectrometry to in situ U–pb zircon geochronology: Chemical Geology, v. 211, no. 1, p. 47–69. [10.1016/j.chemgeo.2004.06.017](https://doi.org/10.1016/j.chemgeo.2004.06.017)
- Jahn, B.M., Griffin, W.L., and Windley, B., 2000, Continental growth in the Phanerozoic: Evidence from central Asia: Tectonophysics, v. 328, no. 1, p. 7–10. [10.1016/S0040-1951\(00\)00174-8](https://doi.org/10.1016/S0040-1951(00)00174-8)
- Jiang, Y.-H., Jiang, S.-Y., Dai, B.-Z., Liao, S.-Y., Zhao, K.-D., and Ling, H.-F., 2009, Middle to late Jurassic felsic and mafic magmatism in southern Hunan province, southeast China: Implications for a continental arc to rifting: Lithos, v. 107, no. 3, p. 185–204. [10.1016/j.lithos.2008.10.006](https://doi.org/10.1016/j.lithos.2008.10.006)
- Ji, W.Q., Wu, F.Y., Chung, S.L., Li, J.X., and Liu, C.Z., 2009, Zircon U–pb geochronology and Hf isotopic constraints on petrogenesis of the Gangdese batholith, southern tibet: Chemical Geology, v. 262, no. 3, p. 229–245. [10.1016/j.chemgeo.2009.01.020](https://doi.org/10.1016/j.chemgeo.2009.01.020)
- Johnson, P.R., Andresen, A., Collins, A.S., Fowler, A.R., Fritz, H., Ghebreab, W., Kusky, T., and Stern, R.J., 2011, Late Cryogenian–Ediacaran history of the Arabian–nubian shield: A review of depositional, plutonic, structural, and tectonic events in the closing stages of the northern east African Orogen: Journal of African Earth Sciences, v. 61, no. 3, p. 167–232. [10.1016/j.jafrearsci.2011.07.003](https://doi.org/10.1016/j.jafrearsci.2011.07.003)
- Karsli, O., Dokuz, A., Uysal, İ., Aydin, F., Chen, B., Kandemir, R., and Wijbrans, J., 2010, Relative contributions of crust and mantle to generation of Campanian high-K calc-alkaline I-type granitoids in a subduction setting, with special reference to the harşit pluton, Eastern Turkey: Contributions to Mineralogy and Petrology, v. 160, no. 4, p. 467–487. [10.1007/s00410-010-0489-z](https://doi.org/10.1007/s00410-010-0489-z)
- Kemp, A.I.S., Hawkesworth, C.J., Foster, G.L., Paterson, B.A., Woodhead, J.D., Hergt, J.M., Gray, C.M., and Whitehouse, M. J., 2007, Magmatic and crustal differentiation history of granitic rocks from Hf–O isotopes in Zircon: Science, v. 315, no. 5814, p. 980–983. [10.1126/science.1136154](https://doi.org/10.1126/science.1136154)
- Kemp, A.I.S., Hawkesworth, C.J., Paterson, B.A., and Kinny, P.D., 2006, Episodic growth of the Gondwana supercontinent from hafnium and oxygen isotopes in zircon: Nature, v. 439, no. 7076, p. 580–583. [10.1038/nature04505](https://doi.org/10.1038/nature04505)
- Khan, A., Faisal, S., Larson, K.P., Robinson, D.M., Ullah, Z., Li, H., and Ur Rehman, H., 2021, New geochronological and geochemical constraints on petrogenesis and tectonic setting of the Loe-Shilman carbonatite complex: Northwest Pakistan: Lithos, v. 404, p. 106497. [10.1016/j.lithos.2021.106497](https://doi.org/10.1016/j.lithos.2021.106497)
- Kinny, P.D., and Maas, R., 2003, Lu–hf and Sm–nd isotope systems in zircon: Reviews in Mineralogy and Geochemistry, v. 53, no. 1, p. 327–341. [10.2113/0530327](https://doi.org/10.2113/0530327)
- Lan, C.Y., Chung, S.L., Jiun-San Shen, J., Lo, C.H., Wang, P.L., Hoa, T.T., Thanh, H.H., and Mertzman, S.A., 2000, Geochemical and Sr–nd isotopic characteristics of granitic rocks from northern Vietnam: Journal of Asian Earth Sciences, v. 18, no. 3, p. 267–280. [10.1016/S1367-9120\(99\)00063-2](https://doi.org/10.1016/S1367-9120(99)00063-2)
- Lan, C.Y., Chung, S.L., Lo, C.H., Lee, T.Y., Wang, P.L., Li, H., and Van Toan, D., 2001, First evidence for Archean continental crust in northern Vietnam and its implications for crustal and tectonic evolution in Southeast Asia: Geology, v. 29, no. 3, p. 219–222. [10.1130/0091-7613\(2001\)029<0219:FEFACC>2.0.CO;2](https://doi.org/10.1130/0091-7613(2001)029<0219:FEFACC>2.0.CO;2)
- Le Fort, P., Cuney, M., Deniel, C., France-Lanord, C., Sheppard, S. M.F., Upreti, B.N., and Vidal, P., 1987, Crustal generation of the Himalayan leucogranites: Tectonophysics, v. 134, no. 1, p. 39–57. [10.1016/0040-1951\(87\)90248-4](https://doi.org/10.1016/0040-1951(87)90248-4)
- Lepvrier, C., Maluski, H., Van Tich, V., Leyreloup, A., Truong Thi, P., and Van Vuong, N., 2004, The Early Triassic Indosinian orogeny in Vietnam (Truong Son Belt and Kontum Massif); implications for the geodynamic evolution of Indochina: Tectonophysics, v. 393, no. 1, p. 87–118. [10.1016/j.tecto.2004.07.030](https://doi.org/10.1016/j.tecto.2004.07.030)
- Likhanov, I.I., and Santosh, M., 2017, Neoproterozoic intraplate magmatism along the western margin of the Siberian Craton: Implications for breakup of the rodnia supercontinent: Precambrian Research, v. 300, p. 315–331. [10.1016/j.precamres.2017.08.019](https://doi.org/10.1016/j.precamres.2017.08.019)
- Li, X.-H., Li, Z.-X., Li, W.-X., Wang, X.-C., and Gao, Y., 2013, Revisiting the “C-type adakites” of the Lower Yangtze River Belt, central eastern China: In-situ zircon Hf–O isotope and geochemical constraints: Chemical Geology, v. 345, p. 1–15. [10.1016/j.chemgeo.2013.02.024](https://doi.org/10.1016/j.chemgeo.2013.02.024)
- Li, X.H., Li, Z.X., Wingate, M.T.D., Chung, S.L., Liu, Y., Lin, G.C., and Li, W.X., 2006, Geochemistry of the 755Ma Mundine well dyke swarm, northwestern Australia: Part of a Neoproterozoic mantle superplume beneath rodnia: Precambrian Research, v. 146, no. 1, p. 1–15. [10.1016/j.precamres.2005.12.007](https://doi.org/10.1016/j.precamres.2005.12.007)
- Li, Z.X., Li, X.H., Zhou, H.W., and Kinny, P.D., 2002, Grenvillian continental collision in South China: New SHRIMP U–Pb zircon results and implications for the configuration of

- rodinia: *Geology*, v. 30, no. 2, p. 163–166. [10.1130/0091-7613\(2002\)030<0163:GCCISC>2.0.CO;2](https://doi.org/10.1130/0091-7613(2002)030<0163:GCCISC>2.0.CO;2)
- Li, X.H., Long, W.G., Li, Q.L., Liu, Y., Zheng, Y.F., Yang, Y.H., Chamberlain, K.R., Wan, D.F., Guo, C.H., Wang, X.C., and Tao, H., 2010, Penglai zircon megacrysts: A potential new working reference material for microbeam determination of Hf–O isotopes and U–pb age: *Geostandards and Geoanalytical Research*, v. 34, no. 2, p. 117–134. [10.1111/j.1751-908X.2010.00036.x](https://doi.org/10.1111/j.1751-908X.2010.00036.x)
- Liu, Y., Hu, Z., Gao, S., Günther, D., Xu, J., Gao, C., and Chen, H., 2008, In situ analysis of major and trace elements of anhydrous minerals by LA-ICP-MS without applying an internal standard: *Chemical Geology*, v. 257, no. 1, p. 34–43. [10.1016/j.chemgeo.2008.08.004](https://doi.org/10.1016/j.chemgeo.2008.08.004)
- Liu, Y., Hu, Z., Zong, K., Gao, C., Gao, S., Xu, J., and Chen, H., 2010, Reappraisal and refinement of zircon U–Pb isotope and trace element analyses by LA-ICP-MS: *Chinese Science Bulletin*, v. 55, no. 15, p. 1535–1546. [10.1007/s11434-010-3052-4](https://doi.org/10.1007/s11434-010-3052-4)
- Li, X.C., Zhao, J.H., Zhou, M.F., Gao, J.F., Sun, W.H., and Tran, M., 2018, Neoproterozoic granitoids from the Phan Si Pan belt, Northwest Vietnam: Implication for the tectonic linkage between Northwest Vietnam and the Yangtze Block: *Precambrian Research*, v. 309, p. 212–230. [10.1016/j.precamres.2017.02.019](https://doi.org/10.1016/j.precamres.2017.02.019)
- Ludwig, K., 2003, User's manual for Isoplot/Ex, version 3.00, a geochronological toolkit for Microsoft excel: Berkeley Geochronology Center Special Publication, v. 4, no. 2, 1–70.
- Luo, T., Hu, Z., Zhang, W., Günther, D., Liu, Y., Zong, K., and Hu, S., 2018, Reassessment of the influence of carrier gases He and Ar on signal intensities in 193 nm excimer LA-ICP-MS analysis: *Journal of Analytical Atomic Spectrometry*, v. 33, no. 10, p. 1655–1663. [10.1039/C8JA00163D](https://doi.org/10.1039/C8JA00163D)
- Luo, T., Hu, Z., Zhang, W., Liu, Y., Zong, K., Zhou, L., Zhang, J., and Hu, S., 2018, Water vapor-assisted “universal” nonmatrix-matched analytical method for the in situ U–pb dating of Zircon, monazite, titanite, and xenotime by laser ablation-inductively coupled plasma mass spectrometry: *Analytical Chemistry*, v. 90, no. 15, p. 9016–9024. [10.1021/acs.analchem.8b01231](https://doi.org/10.1021/acs.analchem.8b01231)
- Mastoi, A.S., Yang, X., Deng, J., Kashani, A.G., and Hakro, A.A.D., 2020, Geochronological and geochemical studies of adakites from Tethyan Belt, Western Pakistan: A clue to geodynamics and Cu–au mineralization: *International Geology Review*, v. 62, no. 10, p. 1273–1293. [10.1080/00206814.2019.1644677](https://doi.org/10.1080/00206814.2019.1644677)
- Maurice, A.E., Bakhit, B.R., Basta, F.F., and Khiamy, A.A., 2013, Geochemistry of gabbros and granitoids (M- and I-types) from the nubian shield of Egypt: Roots of neoproterozoic intra-oceanic island arc: *Precambrian Research*, v. 224, p. 397–411. [10.1016/j.precamres.2012.10.012](https://doi.org/10.1016/j.precamres.2012.10.012)
- Ma, Q., Zheng, J., Griffin, W.L., Zhang, M., Tang, H., Su, Y., and Ping, X., 2012, Triassic “adakitic” rocks in an extensional setting (North China): Melts from the cratonic lower crust: *Lithos*, v. 149, p. 159–173. [10.1016/j.lithos.2012.04.017](https://doi.org/10.1016/j.lithos.2012.04.017)
- Metcalfe, I., 2002, Permian tectonic framework and palaeogeography of SE asia: *Journal of Asian Earth Sciences*, v. 20, no. 6, p. 551–566. [10.1016/S1367-9120\(02\)00022-6](https://doi.org/10.1016/S1367-9120(02)00022-6)
- Metcalfe, I., 2006, Palaeozoic and Mesozoic tectonic evolution and palaeogeography of East Asian crustal fragments: The Korean Peninsula in context: *Gondwana Research*, v. 9, no. 1, p. 24–46. [10.1016/j.gr.2005.04.002](https://doi.org/10.1016/j.gr.2005.04.002)
- Metcalfe, I., 2012, Changhsingian (late permian) conodonts from Son La, northwest Vietnam and their stratigraphic and tectonic implications: *Journal of Asian Earth Sciences*, v. 50, p. 141–149. [10.1016/j.jseas.2012.01.002](https://doi.org/10.1016/j.jseas.2012.01.002)
- Middlemost, E., 1994, Naming materials in the magma/Igneous rock system: *Earth Science Reviews*, v. 37, no. 3–4, p. 215–224. [10.1016/0012-8252\(94\)90029-9](https://doi.org/10.1016/0012-8252(94)90029-9)
- Miller, C.F., 1985, Are strongly peraluminous magmas derived from pelitic sedimentary sources?: *The Journal of Geology*, v. 93, no. 6, p. 673–689. [10.1086/628995](https://doi.org/10.1086/628995)
- Minh, P., Hieu, P.T., and Hoang, N.K., 2018, Geochemical and geochronological studies of the muong hum alkaline granitic pluton from the Phan Si Pan Zone, northwest Vietnam: Implications for petrogenesis and tectonic setting: *The Island Arc*, v. 27, no. 4, p. 12250. [10.1111/iar.12250](https://doi.org/10.1111/iar.12250)
- Minh, P., Hieu, P.T., Thuy, N.T.B., Dung, L., Kawaguchi, K., and Dung, P.T., 2021, Neoproterozoic granitoids from the Phan Si Pan Zone, NW Vietnam: Geochemistry and geochronology constraints on reconstructing South China–India Palaeogeography: *International Geology Review*, v. 63, no. 5, p. 585–600. [10.1080/00206814.2020.1728584](https://doi.org/10.1080/00206814.2020.1728584)
- Moghadam, H.S., Khademi, M., Hu, Z., Stern, R.J., Santos, J.F., and Wu, Y., 2015, Cadomian (Ediacaran–Cambrian) arc magmatism in the ChahJam–biarjmand metamorphic complex (Iran): Magmatism along the northern active margin of Gondwana: *Gondwana Research*, v. 27, no. 1, p. 439–452. [10.1016/j.gr.2013.10.014](https://doi.org/10.1016/j.gr.2013.10.014)
- Nam, T., Daihoc, K., and Nguyen, H., 2003, 750 ma U–Pb zircon age of the Po sen complex and tectonic implication: *Journal of Geology*, v. 274, p. 11–16.
- Patiño Douce, A.E., 1999, What do experiments tell us about the relative contributions of crust and mantle to the origin of granitic magmas?: Geological Society, London, Special Publications, v. 168, no. 1, p. 55–75. [10.1144/GSL.SP.1999.168.01.05](https://doi.org/10.1144/GSL.SP.1999.168.01.05)
- Pearce, J.A., Harris, N.B., and Tindle, A.G., 1984, Trace element discrimination diagrams for the tectonic interpretation of granitic rocks: *Journal of Petrology*, v. 25, p. 956–983. [10.1093/petrology/25.4.956](https://doi.org/10.1093/petrology/25.4.956)
- Peccerillo, A., and Taylor, S., 1976, Geochemistry of eocene calc-alkaline volcanic rocks from the Kastamonu area, northern Turkey: *Contributions to Mineralogy and Petrology*, v. 58, no. 1, p. 63–81. [10.1007/BF00384745](https://doi.org/10.1007/BF00384745)
- Pereira, M.F., Castro, A., and Fernández, C., 2015, The inception of a paleotethyan magmatic arc in Iberia: *Geoscience Frontiers*, v. 6, no. 2, p. 297–306. [10.1016/j.gsf.2014.02.006](https://doi.org/10.1016/j.gsf.2014.02.006)
- Peytcheva, I., von Quadt, A., Georgiev, N., Ivanov, Z., Heinrich, C. A., and Frank, M., 2008, Combining trace-element compositions, U–pb geochronology and Hf isotopes in zircons to unravel complex calcalkaline magma chambers in the upper cretaceous srednogorie zone (Bulgaria): *Lithos*, v. 104, no. 1, p. 405–427. [10.1016/j.lithos.2008.01.004](https://doi.org/10.1016/j.lithos.2008.01.004)
- Pham, T.H., Chen, F., Me, L.T., Thuy, N.T.B., Siebel, W., and Lan, T.-G., 2012, Zircon U–pb ages and Hf isotopic compositions from the sin quyen formation: The Precambrian crustal evolution of northwest Vietnam: *International Geology Review*, v. 54, no. 13, p. 1548–1561. [10.1080/00206814.2011.646831](https://doi.org/10.1080/00206814.2011.646831)
- Pham, T.H., Chen, F.K., Thuy, N.T.B., Quốc Cu'ờng, N., and Li, S. Q., 2013, Geochemistry and zircon U–pb ages and Hf isotopic composition of Permian alkali granitoids of the Phan Si

- Pan zone in northwestern Vietnam: *Journal of Geodynamics*, v. 69, p. 106–121. [10.1016/j.jog.2012.03.002](https://doi.org/10.1016/j.jog.2012.03.002)
- Pham, T.H., Chen, F., Wang, W., Nguyen, T., Bui, M., and Nguyen, Q., 2009, Zircon U-Pb ages and Hf isotopic composition of the Posen granite in northwest Vietnam: *Acta Petrologica Sinica*, v. 25, p. 3141–3152. (in Chinese with English abstract).
- Pham, T.H., Lei, W.X., Minh, P., Thuy, N.T.B., Phuc, L.D., and Luyen, N.D., 2022, Archean to paleoproterozoic crustal evolution in the Phan Si Pan zone, Northwest Vietnam: Evidence from the U-Pb geochronology and Sr-nd-hf isotopic geochemistry: *International Geology Review*, v. 64, no. 1, p. 96–118. [10.1080/00206814.2020.1839976](https://doi.org/10.1080/00206814.2020.1839976)
- Pham, T.T., Shellnutt, J.G., Tran, T.-A., and Lee, H.-Y., 2020, Petrogenesis of eocene to early Oligocene granitic rocks in Phan Si Pan uplift area, northwestern Vietnam: Geochemical implications for the Cenozoic crustal evolution of the South China block: *Lithos*, v. 372, p. 105640. [10.1016/j.lithos.2020.105640](https://doi.org/10.1016/j.lithos.2020.105640)
- Piper, J.D.A., 2007, The Neoproterozoic supercontinent Palaeopangaea: *Gondwana Research*, v. 12, no. 3, p. 202–227. [10.1016/j.gr.2006.10.014](https://doi.org/10.1016/j.gr.2006.10.014)
- Polyakov, G., Balykin, P., Hoa, T.T., Phuong, N.T., Thanh, H.H., Hung, C., Ponomarchuk, V., Lebedev, Y.N., and Kireev, A., 1998, Evolution of the Mesozoic-Cenozoic magmatism of the Song Da rift and its contouring structures: *Geologiya i Geofizika*, v. 39, no. 6, 695–706.
- Qian, Q., and Hermann, J., 2010, Formation of high-mg diorites through assimilation of peridotite by monzodiorite magma at crustal depths: *Journal of Petrology*, v. 51, no. 7, p. 1381–1416. [10.1093/petrology/egq023](https://doi.org/10.1093/petrology/egq023)
- Qian, Q., and Hermann, J., 2013, Partial melting of lower crust at 10–15 kbar: Constraints on adakite and TTG formation: *Contributions to Mineralogy and Petrology*, v. 165, no. 6, p. 1195–1224. [10.1007/s00410-013-0854-9](https://doi.org/10.1007/s00410-013-0854-9)
- Qi, L., Hu, J., and Gregoire, D.C., 2000, Determination of trace elements in granites by inductively coupled plasma mass spectrometry: *Talanta*, v. 51, no. 3, p. 507–513. [10.1016/S0039-9140\(99\)00318-5](https://doi.org/10.1016/S0039-9140(99)00318-5)
- Qi, X., Santosh, M., Zhao, Y., Hu, Z., Zhang, C., Ji, F., and Wei, C., 2016, Mid-neoproterozoic ridge subduction and magmatic evolution in the northeastern margin of the Indochina block: Evidence from geochronology and geochemistry of calc-alkaline plutons: *Lithos*, v. 248–251, p. 138–152.
- Qi, X., Santosh, M., Zhu, L., Zhao, Y., Hu, Z., Zhang, C., and Ji, F., 2014, Mid-neoproterozoic arc magmatism in the northeastern margin of the Indochina block, SW China: Geochronological and petrogenetic constraints and implications for Gondwana assembly: *Precambrian Research*, v. 245, p. 207–224. [10.1016/j.precamres.2014.02.008](https://doi.org/10.1016/j.precamres.2014.02.008)
- Qi, X., Zeng, L., Zhu, L., Hu, Z., and Hou, K., 2012, Zircon U–pb and Lu–hf isotopic systematics of the daping plutonic rocks: Implications for the neoproterozoic tectonic evolution of the northeastern margin of the Indochina block: *Southwest China: Gondwana Research*, v. 21, no. 1, p. 180–193. [10.1016/j.gr.2011.06.004](https://doi.org/10.1016/j.gr.2011.06.004)
- Qi, H., Zhao, J.-H., and Johnson, T.E., 2023, The fundamental role of H₂O in the generation of Coeval Sodic and potassic granitoids at continental arcs: An example from the Yangtze Block: South China: *Journal of Petrology*, v. 64, no. 5, p. 1–24. [10.1093/petrology/egad024](https://doi.org/10.1093/petrology/egad024)
- Rehman, H.U., Khan, T., Lee, H.-Y., Chung, S.-L., Jan, M.Q., Zafar, T., and Murata, M., 2021, Petrogenetic source and tectonic evolution of the neoproterozoic nagar parkar igneous complex granitoids: Evidence from zircon Hf isotope and trace element geochemistry: *Precambrian Research*, v. 354, p. 106047. [10.1016/j.precamres.2020.106047](https://doi.org/10.1016/j.precamres.2020.106047)
- Roberts, M.P., and Clemens, J.D., 1993, Origin of high-potassium, calc-alkaline, I-type granitoids: *Geology*, v. 21, no. 9, p. 825–828. [10.1130/0091-7613\(1993\)021<0825:OOHPTA>2.3.CO;2](https://doi.org/10.1130/0091-7613(1993)021<0825:OOHPTA>2.3.CO;2)
- Sajid, M., Andersen, J., Rocholl, A., and Wiedenbeck, M., 2018, U-Pb geochronology and petrogenesis of peraluminous granitoids from northern Indian plate in NW Pakistan: Andean type orogenic signatures from the early Paleozoic along the northern Gondwana: *Lithos*, v. 318, p. 340–356. [10.1016/j.lithos.2018.08.024](https://doi.org/10.1016/j.lithos.2018.08.024)
- Santosh, M., Xiao, W.J., Tsunogae, T., Chetty, T.R.K., and Yellappa, T., 2012, The Neoproterozoic subduction complex in southern India: SIMS zircon U–pb ages and implications for Gondwana assembly: *Precambrian Research*, v. 192–195, p. 190–208. [10.1016/j.precamres.2011.10.025](https://doi.org/10.1016/j.precamres.2011.10.025)
- Santosh, M., Yang, Q.Y., Shaji, E., Tsunogae, T., Mohan, M.R., and Satyanarayanan, M., 2015, An exotic mesoarchean microcontinent: The coorg block, southern India: *Gondwana Research*, v. 27, no. 1, p. 165–195. [10.1016/j.gr.2013.10.005](https://doi.org/10.1016/j.gr.2013.10.005)
- Sheldrick, T.C., Barry, T.L., Millar, I.L., Barfod, D.N., Halton, A.M., and Smith, D.J., 2020, Evidence for southward subduction of the mongol-okhotsk oceanic plate: Implications from Mesozoic adakitic lavas from Mongolia: *Gondwana Research*, v. 79, p. 140–156. [10.1016/j.gr.2019.09.007](https://doi.org/10.1016/j.gr.2019.09.007)
- Shu, L.S., Faure, M., Yu, J.H., and Jahn, B.M., 2011, Geochronological and geochemical features of the cathaysia block (South China): New evidence for the Neoproterozoic breakup of rodinia: *Precambrian Research*, v. 187, no. 3–4, p. 263–276. [10.1016/j.precamres.2011.03.003](https://doi.org/10.1016/j.precamres.2011.03.003)
- Sisson, T.W., Ratajeski, K., Hankins, W.B., and Glazner, A.F., 2005, Voluminous granitic magmas from common basaltic sources: Contributions to Mineralogy and Petrology, v. 148, no. 6, p. 635–661. [10.1007/s00410-004-0632-9](https://doi.org/10.1007/s00410-004-0632-9)
- Sláma, J., Košler, J., Condon, D.J., Crowley, J.L., Gerdes, A., Hanchar, J.M., Horstwood, M.S.A., Morris, G.A., Nasdala, L., Norberg, N., Schaltegger, U., Schoene, B., Tubrett, M.N., and Whitehouse, M.J., 2008, Plešovice zircon — A new natural reference material for U–Pb and Hf isotopic microanalysis: *Chemical Geology*, v. 249, no. 1, p. 1–35. [10.1016/j.chemgeo.2007.11.005](https://doi.org/10.1016/j.chemgeo.2007.11.005)
- Sreejith, C., and Kumar, G.R., 2013, Petrogenesis of high-K metagranites in the Kerala Khondalite Belt, southern India: A possible magmatic-arc link between India, Sri Lanka, and Madagascar: *Journal of Geodynamics*, v. 63, p. 69–82. [10.1016/j.jog.2012.10.002](https://doi.org/10.1016/j.jog.2012.10.002)
- Sun, S.S., and McDonough, W.F., 1989, Chemical and isotopic systematics of oceanic basalts: Implications for mantle composition and processes: Geological society of London: Geological Society, London, Special Publications, v. 42, no. 1, p. 313–345. [10.1144/GSL.SP.1989.042.01.19](https://doi.org/10.1144/GSL.SP.1989.042.01.19)
- Tapponnier, P., Lacassin, R., Leloup, P.H., Schärer, U., Dalai, Z., Haiwei, W., and Jiayou, Z., 1990, The Ailao Shan/Red River metamorphic belt: Tertiary left-lateral shear between Indochina and South China: *Nature*, v. 343, no. 6257, p. 431–437. [10.1038/343431a0](https://doi.org/10.1038/343431a0)

- Thomas, R.J., De Waele, B., Schofield, D.I., Goodenough, K.M., Horstwood, M., Tucker, R., Bauer, W., Annells, R., Howard, K., Walsh, G., Rabarimanana, M., Rafahatelo, J.M., Ralison, A.V., and Randriamananjara, T., 2009, Geological evolution of the Neoproterozoic Bemarivo Belt, northern Madagascar: *Precambrian Research*, v. 172, no. 3, p. 279–300. [10.1016/j.precamres.2009.04.008](https://doi.org/10.1016/j.precamres.2009.04.008)
- Tran, T.H., Lan, C.-Y., Usuki, T., Shellnutt, J.G., Pham, T.D., Tran, T. A., Pham, N.C., Ngo, T.P., Izokh, A.E., and Borisenko, A.S., 2015, Petrogenesis of late permian silicic rocks of Tu Le basin and Phan Si Pan uplift (NW Vietnam) and their association with the Emeishan large igneous province: *Journal of Asian Earth Sciences*, v. 109, p. 1–19. [10.1016/j.jseae.2015.05.009](https://doi.org/10.1016/j.jseae.2015.05.009)
- Usuki, T., Lan, C.-Y., Tran, T.H., Pham, T.D., Wang, K.-L., Shellnutt, G.J., and Chung, S.-L., 2015, Zircon U–pb ages and Hf isotopic compositions of alkaline silicic magmatic rocks in the Phan Si Pan-tu Le region, northern Vietnam: Identification of a displaced western extension of the Emeishan large igneous province: *Journal of Asian Earth Sciences*, v. 97, p. 102–124. [10.1016/j.jseae.2014.10.016](https://doi.org/10.1016/j.jseae.2014.10.016)
- Valley, J.W., Lackey, J.S., Cavosie, A.J., Clechenko, C.C., Spicuzza, M.J., Basei, M.A.S., Bindeman, I.N., Ferreira, V.P., Sial, A.N., King, E.M., Peck, W.H., Sinha, A.K., and Wei, C.S., 2005, 4.4 billion years of crustal maturation: Oxygen isotope ratios of magmatic zircon: *Contributions to Mineralogy and Petrology*, v. 150, no. 6, p. 561–580. [10.1007/s00410-005-0025-8](https://doi.org/10.1007/s00410-005-0025-8)
- Van Lente, B., Ashwal, L.D., Pandit, M.K., Bowring, S.A., and Torsvik, T.H., 2009, Neoproterozoic hydrothermally altered basaltic rocks from Rajasthan, northwest India: Implications for late Precambrian tectonic evolution of the Aravalli Craton: *Precambrian Research*, v. 170, no. 3, p. 202–222. [10.1016/j.precamres.2009.01.007](https://doi.org/10.1016/j.precamres.2009.01.007)
- Villaseca, C., Orejana, D., and Belousova, E.A., 2012, Recycled metaigneous crustal sources for S- and I-type Variscan granitoids from the Spanish Central System batholith: Constraints from Hf isotope zircon composition: *Lithos*, v. 153, p. 84–93. [10.1016/j.lithos.2012.03.024](https://doi.org/10.1016/j.lithos.2012.03.024)
- Wang, W., Cawood, P.A., Zhou, M.-F., and Zhao, J.-H., 2016, Paleoproterozoic magmatic and metamorphic events link Yangtze to northwest Laurentia in the Nuna supercontinent: *Earth and Planetary Science Letters*, v. 433, p. 269–279. [10.1016/j.epsl.2015.11.005](https://doi.org/10.1016/j.epsl.2015.11.005)
- Wang, X.C., Li, X.H., Li, W.X., and Li, Z.X., 2009, Variable involvements of mantle plumes in the genes of mid-Neoproterozoic basaltic rocks in South China: A review: *Gondwana Research*, v. 15, no. 3–4, p. 381–395. [10.1016/j.gr.2008.08.003](https://doi.org/10.1016/j.gr.2008.08.003)
- Wang, P.-L., Lo, C.-H., Lan, C.-Y., Chung, S.-L., Lee, T.-Y., Nam, T. N., and Sano, Y., 2011, Thermochronology of the PoSen complex, northern Vietnam: Implications for tectonic evolution in SE Asia: *Journal of Asian Earth Sciences*, v. 40, no. 5, p. 1044–1055. [10.1016/j.jseae.2010.11.006](https://doi.org/10.1016/j.jseae.2010.11.006)
- Wang, H., Wu, Y.-B., Qin, Z.-W., Zhu, L.-Q., Liu, Q., Liu, X.-C., Gao, S., Wijbrans, J.R., Zhou, L., Gong, H.-J., and Yuan, H.-L., 2013, Age and geochemistry of Silurian gabbroic rocks in the Tongbai orogen, central China: Implications for the geodynamic evolution of the North Qinling arc–back-arc system: *Lithos*, v. 179, p. 1–15. [10.1016/j.lithos.2013.07.021](https://doi.org/10.1016/j.lithos.2013.07.021)
- Wang, Y., Zhou, Y., Cai, Y., Liu, H., Zhang, Y., and Fan, W., 2016, Geochronological and geochemical constraints on the petrogenesis of the Ailaoshan granitic and migmatite rocks and its implications on Neoproterozoic subduction along the SW yangtze block: *Precambrian Research*, v. 283, p. 106–124. [10.1016/j.precamres.2016.07.017](https://doi.org/10.1016/j.precamres.2016.07.017)
- Weissman, A., Kessel, R., Navon, O., and Stein, M., 2013, The petrogenesis of calc-alkaline granites from the elat massif, northern Arabian–Nubian shield: *Precambrian Research*, v. 236, p. 252–264. [10.1016/j.precamres.2013.07.005](https://doi.org/10.1016/j.precamres.2013.07.005)
- White, A.J.R., Chappell, B.W., 1983, Granitoid types and their distribution in the Lachlan Fold Belt, southeastern Australia, in Roddick, J.A., ed., *Circum-Pacific Plutonic Terranes*, Geological Society of America, v. 159, p. 21–34. [10.1130/MEM159-p21](https://doi.org/10.1130/MEM159-p21)
- Wiedenbeck, M., Alle, P., Corfu, F., Griffin, W.L., Meier, M., Oberli, F.V., Quadt, A.V., Roddick, J., and Spiegel, W., 1995, Three natural zircon standards for U–Th–Pb, Lu–Hf, trace element and REE analyses: *Geostandards Newsletter*, v. 19, no. 1, p. 1–23. [10.1111/j.1751-908X.1995.tb00147.x](https://doi.org/10.1111/j.1751-908X.1995.tb00147.x)
- Wolf, M.B., and Wyllie, P.J., 1994, Dehydration-melting of amphibolite at 10 kbar: The effects of temperature and time: *Contributions to Mineralogy and Petrology*, v. 115, no. 4, p. 369–383. [10.1007/BF00320972](https://doi.org/10.1007/BF00320972)
- Wu, Y.-B., Gao, S., Zhang, H.-F., Yang, S.-H., Jiao, W.-F., Liu, Y.-S., and Yuan, H.-L., 2008, Timing of UHP metamorphism in the Hong'an area, western Dabie Mountains, China: Evidence from zircon U–pb age, trace element and Hf isotope composition: *Contributions to Mineralogy and Petrology*, v. 155, no. 1, p. 123–133. [10.1007/s00410-007-0231-7](https://doi.org/10.1007/s00410-007-0231-7)
- Wu, F.-Y., Yang, Y.-H., Xie, L.-W., Yang, J.-H., and Xu, P., 2006, Hf isotopic compositions of the standard zircons and baddeleyites used in U–pb geochronology: *Chemical Geology*, v. 234, no. 1–2, p. 105–126. [10.1016/j.chemgeo.2006.05.003](https://doi.org/10.1016/j.chemgeo.2006.05.003)
- Wu, Y., and Zheng, Y., 2004, Genesis of zircon and its constraints on interpretation of U–Pb age: *Chinese Science Bulletin*, v. 49, no. 15, p. 1554–1569. [10.1007/BF03184122](https://doi.org/10.1007/BF03184122)
- Xiao, L., and Clemens, J.D., 2007, Origin of potassic (C-type) adakite magmas: Experimental and field constraints: *Lithos*, v. 95, no. 3–4, p. 399–414. [10.1016/j.lithos.2006.09.002](https://doi.org/10.1016/j.lithos.2006.09.002)
- Xiong, F., Zhong, H., Huang, H., Liu, X., and Hou, M., 2023, Petrogenetic and tectonic implications of Neoproterozoic igneous rocks from the western Yangtze Block, South China: *Precambrian Research*, v. 387, p. 106977.
- Xu, P., Wu, F., Xie, L., and Yang, Y., 2004, Hf isotopic compositions of the standard zircons for U–Pb dating: *Chinese Science Bulletin*, v. 49, no. 15, p. 1642–1648. [10.1007/BF03184136](https://doi.org/10.1007/BF03184136)
- Xu, J., Xia, X.P., Yin, C.Q., Spencer, C.J., Lai, C.K., Zhang, L., and Cui, Z.X., 2022, Geochronology and geochemistry of the granitoids in the Diancangshan–Ailaoshan fold belt: Implications on the Neoproterozoic subduction and crustal melting along the southwestern Yangtze Block, South China: *Precambrian Research*, v. 383, p. 106907. [10.1016/j.precamres.2022.106907](https://doi.org/10.1016/j.precamres.2022.106907)
- Yang, Q., Santosh, M., Shen, J., and Li, S., 2014, Juvenile vs. recycled crust in NE China: Zircon U–pb geochronology, Hf isotope and an integrated model for Mesozoic gold mineralization in the Jiaodong Peninsula: *Gondwana Research*, v. 25, no. 4, p. 1445–1468. [10.1016/j.gr.2013.06.003](https://doi.org/10.1016/j.gr.2013.06.003)
- Yang, Y.-N., Wang, X.-C., Li, Q.-L., and Li, X.-H., 2016, Integrated in situ U–pb age and Hf–O analyses of zircon from Suixian Group in northern Yangtze: New insights into the Neoproterozoic low- $\delta^{18}\text{O}$ magmas in the South China block: *Precambrian Research*, v. 273, p. 151–164. [10.1016/j.precamres.2015.12.008](https://doi.org/10.1016/j.precamres.2015.12.008)

- Yuan, H.-L., Gao, S., Dai, M.-N., Zong, C.-L., Günther, D., Fontaine, G.H., Liu, X.-M., and Diwu, C., 2008, Simultaneous determinations of U–pb age, Hf isotopes and trace element compositions of zircon by excimer laser-ablation quadrupole and multiple-collector ICP-MS: *Chemical Geology*, v. 247, no. 1, p. 100–118. [10.1016/j.chemgeo.2007.10.003](https://doi.org/10.1016/j.chemgeo.2007.10.003)
- Yu, J.H., O'Reilly, S.Y., Wang, L., Griffin, W.L., Zhang, M., Wang, R., Jiang, S., and Shu, L., 2008, Where was South China in the rodinia supercontinent? Evidence from U–Pb geochronology and Hf isotopes of detrital zircons: *Precambrian Research*, v. 164, no. 1–2, p. 1–15. [10.1016/j.precamres.2008.03.002](https://doi.org/10.1016/j.precamres.2008.03.002)
- Żelaźniewicz, A., Hòà, T.T., and Larionov, A.N., 2013, The significance of geological and zircon age data derived from the wall rocks of the Ailao Shan–Red River Shear Zone: NW Vietnam: *Journal of Geodynamics*, v. 69, p. 122–139. [10.1016/j.jog.2012.04.002](https://doi.org/10.1016/j.jog.2012.04.002)
- Zhao, G., and Cawood, P.A., 2012, Precambrian geology of China: *Precambrian Research*, v. 222–223, p. 13–54.
- Zhao, T., Cawood, P.A., Wang, K., Zi, J.W., Feng, Q., Nguyen, Q. M., and Tran, D.M., 2019, Neoproterozoic K-rich granites in the Phan Si Pan Complex, North Vietnam: Constraints on the early crustal evolution of the Yangtze Block: *Precambrian Research*, v. 332, p. 105395. [10.1016/j.precamres.2019.105395](https://doi.org/10.1016/j.precamres.2019.105395)
- Zhao, T., Cawood, P.A., Zi, J.W., Wang, K., Feng, Q., Nguyen, Q. M., and Tran, D.M., 2019, Early paleoproterozoic magmatism in the Yangtze Block: Evidence from zircon U–Pb ages, Sr–Nd–Hf isotopes and geochemistry of ca. 2.3 Ga and 2.1 Ga granitic rocks in the Phan Si Pan Complex, North Vietnam: *Precambrian Research*, v. 324, p. 253–268. [10.1016/j.precamres.2019.01.012](https://doi.org/10.1016/j.precamres.2019.01.012)
- Zhao, T., Cawood, P.A., Zi, J.W., Wang, K., Feng, Q., Tran, D.M., Nguyen, Q.M., Dang, C.M., and Nguyen, Q.M., 2023, Positioning the Yangtze Block within Nuna: Constraints from paleoproterozoic granitoids in North Vietnam: *Precambrian Research*, v. 391, p. 107059. [10.1016/j.precamres.2023.107059](https://doi.org/10.1016/j.precamres.2023.107059)
- Zhao, T., Li, J., Liu, G., Cawood, P.A., Zi, J.W., Wang, K., Feng, Q., Hu, S., Zeng, W., and Zhang, H., 2020, Petrogenesis of Archean TTGs and potassic granites in the southern Yangtze Block: Constraints on the early formation of the Yangtze Block: *Precambrian Research*, v. 347, p. 105848. [10.1016/j.precamres.2020.105848](https://doi.org/10.1016/j.precamres.2020.105848)
- Zhao, J.-H., Nebel, O., and Johnson, T.E., 2021, Formation and evolution of a Neoproterozoic Continental Magmatic Arc: *Journal of Petrology*, v. 62, no. 8, p. 1–53. [10.1093/petrology/egab029](https://doi.org/10.1093/petrology/egab029)
- Zhao, J.H., and Zhou, M.F., 2007, Neoproterozoic adakitic plutons and arc magmatism along the western margin of the Yangtze Block, South China: *The Journal of Geology*, v. 115, no. 6, p. 675–689. [10.1086/521610](https://doi.org/10.1086/521610)
- Zhao, J.-H., and Zhou, M.-F., 2008, Neoproterozoic adakitic plutons in the northern margin of the Yangtze Block, China: Partial melting of a thickened lower crust and implications for secular crustal evolution: *Lithos*, v. 104, no. 1, p. 231–248. [10.1016/j.lithos.2007.12.009](https://doi.org/10.1016/j.lithos.2007.12.009)
- Zhao, J.-H., Zhou, M.-F., Yan, D.-P., Zheng, J.-P., and Li, J.-W., 2011, Reappraisal of the ages of Neoproterozoic strata in South China: No connection with the Grenvillian orogeny: *Geology*, v. 39, no. 4, p. 299–302. [10.1130/G31701.1](https://doi.org/10.1130/G31701.1)
- Zheng, J., Griffin, W., O'Reilly, S.Y., Zhang, M., Pearson, N., and Pan, Y., 2006, Widespread Archean basement beneath the Yangtze craton: *Geology*, v. 34, no. 6, p. 417–420. [10.1130/G22282.1](https://doi.org/10.1130/G22282.1)
- Zheng, Y.-F., Wu, R.-X., Wu, Y.-B., Zhang, S.-B., Yuan, H., and Wu, F.-Y., 2008, Rift melting of juvenile arc-derived crust: Geochemical evidence from Neoproterozoic volcanic and granitic rocks in the Jiangnan Orogen, South China: *Precambrian Research*, v. 163, no. 3, p. 351–383. [10.1016/j.precamres.2008.01.004](https://doi.org/10.1016/j.precamres.2008.01.004)
- Zhou, M.F., Ma, Y., Yan, D.P., Xia, X., Zhao, J.H., and Sun, M., 2006, The Yanbian terrane (Southern Sichuan Province, SW China): A Neoproterozoic arc assemblage in the western margin of the Yangtze block: *Precambrian Research*, v. 144, no. 1–2, p. 19–38. [10.1016/j.precamres.2005.11.002](https://doi.org/10.1016/j.precamres.2005.11.002)
- Zhou, M.F., Yan, D.P., Kennedy, A.K., Li, Y., and Ding, J., 2002, SHRIMP U–pb zircon geochronological and geochemical evidence for Neoproterozoic arc-magmatism along the western margin of the Yangtze Block, South China: *Earth and Planetary Science Letters*, v. 196, no. 1–2, p. 51–67. [10.1016/S0012-821X\(01\)00595-7](https://doi.org/10.1016/S0012-821X(01)00595-7)
- Zhou, M.F., Yan, D.P., Wang, C.L., Qi, L., and Kennedy, A., 2006, Subduction-related origin of the 750 ma xuelongbao adakitic complex (Sichuan Province, China): Implications for the tectonic setting of the giant Neoproterozoic magmatic event in South China: *Earth and Planetary Science Letters*, v. 248, no. 1–2, p. 286–300. [10.1016/j.epsl.2006.05.032](https://doi.org/10.1016/j.epsl.2006.05.032)
- Zhou, X., Yu, J.H., Sun, T., Wang, X., Tran, M., and Nguyen, D., 2020, Does neoproterozoic nam Co formation in Northwest Vietnam belong to South China or Indochina?: *Precambrian Research*, v. 337, p. 105556. [10.1016/j.precamres.2019.105556](https://doi.org/10.1016/j.precamres.2019.105556)
- Zhu, Y., Lai, S., Qin, J., Zhu, R., Zhang, F., and Zhang, Z., 2019, Geochemistry and zircon U–pb–Hf isotopes of the 780 ma I-type granites in the western Yangtze Block: Petrogenesis and crustal evolution: *International Geology Review*, v. 61, no. 10, p. 1222–1243. [10.1080/00206814.2018.1504330](https://doi.org/10.1080/00206814.2018.1504330)
- Zhu, R.Z., Lai, S.C., Santosh, M., Qin, J.F., and Zhao, S.W., 2017, Early Cretaceous Na-rich granitoids and their enclaves in the Tengchong Block, SW China: Magmatism in relation to subduction of the bangong–nujiang Tethys ocean: *Lithos*, v. 286, p. 175–190. [10.1016/j.lithos.2017.05.017](https://doi.org/10.1016/j.lithos.2017.05.017)
- Zhu, D.C., Mo, X.X., Niu, Y., Zhao, Z.-D., Wang, L.Q., Liu, Y.S., and Wu, F.Y., 2009, Geochemical investigation of early cretaceous igneous rocks along an east–west traverse throughout the central Lhasa Terrane, Tibet: *Chemical Geology*, v. 268, no. 3, p. 298–312. [10.1016/j.chemgeo.2009.09.008](https://doi.org/10.1016/j.chemgeo.2009.09.008)
- Zhu, D.C., Mo, X.X., Niu, Y., Zhao, Z.D., Wang, L.Q., Pan, G.T., and Wu, F.Y., 2009, Zircon U–pb dating and in-situ Hf isotopic analysis of permian peraluminous granite in the Lhasa terrane, southern Tibet: Implications for permian collisional orogeny and paleogeography: *Tectonophysics*, v. 469, no. 1, p. 48–60. [10.1016/j.tecto.2009.01.017](https://doi.org/10.1016/j.tecto.2009.01.017)
- Zou, H., Li, Q.L., Bagas, L., Wang, X.C., Chen, A.Q., and Li, X. H., 2021, A neoproterozoic low- $\delta^{18}\text{O}$ magmatic ring around South China: Implications for configuration and breakup of rodinia supercontinent: *Earth and Planetary Science Letters*, v. 575, p. 117196. [10.1016/j.epsl.2021.117196](https://doi.org/10.1016/j.epsl.2021.117196)